

Remote Sensing Based Water Productivity Assessment – Sri Lanka (Part A)



FINAL REPORT

Final Project Report submitted to ADB under the program for Expanding Support to Water Accounting in River Basins and Water Productivity in Irrigation Schemes.

Citation: Velpuri, N.M., Khan, A., and Rebelo, L-M., 2020. Remote Sensing Based Water Productivity Assessment – Final Project Report, Northwestern and Uva Provinces, Sri Lanka; IWMI, Colombo, Sri Lanka

Cover image: Irrigated crops, Saaliya Thilakaratne / IWMI

**EXPANDING SUPPORT TO WATER ACCOUNTING IN RIVER
BASINS AND WATER PRODUCTIVITY IN IRRIGATION SCHEMES**

**Project final report:
Remote Sensing Based Water
Productivity Assessment, Sri Lanka
(Part A)**

**PREPARED FOR THE
ASIAN DEVELOPMENT BANK
BY**

The International Water Management Institute

October 2020

TABLE OF CONTENTS

I. INTRODUCTION	1
II. PROJECT BACKGROUND.....	1
III. SCOPE OF SERVICES	2
IV. VEGETATION GROWTH AND WATER DEFICIT ASSESSMENT.....	4
A. Background: Site Description	4
B. Summary of the approach	7
1. Analysis of irrigated crop phenology	7
2. Water Deficit Analysis	9
C. pySEBAL Implementation.....	10
1. Data inputs	10
2. Cloud masking and gap filling	15
3. Water Deficits and Biomass Production	16
D. Presentation of Results	17
1. Analysis of irrigated crop phenology	17
2. Crop Water Consumption.....	21
3. Relative Water Deficit	25
4. Above Ground Biomass Production	28
V. SUMMARY AND KEY FINDINGS	32
VI. REFERENCES	34

LIST OF FIGURES

Figure 1: Topography of Sri Lanka along with the boundaries of the 25 basins to be analysed, with the four which have been identified as priorities for investment highlighted in red (Source: SRTM and IWMI estimates).	5
Figure 2. Distribution of average monthly rainfall (P) and potential evapotranspiration (ET _p) for the 25 basins during 2014-2018; a) absolute monthly estimates of P and ET _p ; b) cumulative estimates of P and ET _p , and, c) the water balance (P–ET _p).	6
Figure 3. A flowchart showing the describing the processing steps for the phenology analysis for the 25 river basins.....	7
Figure 4: Data used for the phenology analysis; a) Mean NDVI over 2000-2018 with basin boundaries; b) Irrigated crop map (IWMI, 2013) and c) Mean NDVI for the irrigated areas. ..	8
Figure 5: Illustration of phenology parameters (start of season, SOS; end of season, EOS and length of season (LOS)) for irrigated rice fields in Sri Lanka derived from the time-series of NDVI data. SOS, EOS and LOS are shown as day of the year.	9
Figure 6: Cloud cover percentage during Maha and Yala growing seasons for the two northern (Mi Oya and Deduru Oya), and the two southern (Kirindi Oya and Menik Ganga) river basins	13
Figure 7: Map of irrigated areas for the four basins (Left panel Kirindi Oya and Menik Ganga, right panel Mi Oya and Deduru Oya; Source: IWMI 2013).....	15
Figure 8: The pySEBAL methodological framework (Source: IHE Delft and IWMI, 2020)....	15
Figure 9: Mean NDVI time-series for the Mi Oya basin (2000-2018) showing the Maha and Yala cropping seasons separated by an insignificant change in NDVI profile, thus representing an unimodal curve.	18
Figure 10. Mean NDVI profile in Karanda Oya Basin showing absence of distinct seasonal changes in NDVI.	18
Figure 11. Presence of tree cover in and around irrigated fields in the Karanda Oya basin. The grid represents the 250 m irrigated pixels. The location of Karanda Oya basin is shown in the left panel in cyan; the black dot indicates the location of the grids.	19
Figure 12: Deviation from the mean for each of the crop phenology parameters analysed: Start of season (SOS), End of season (EOS) and Length of season (LOS) for the cropping seasons (Maha + Yala) in the Kirindi Oya basin, Sri Lanka over the period 2000 – 2018.	20
Figure 13: Spatiotemporal distribution of seasonal ET _a during the Maha season in the Mi Oya and Deduru Oya.....	22
Figure 14: Spatiotemporal distribution of seasonal ET _a during the Yala seasons in Mi Oya and Deduru Oya.....	23
Figure 15: Spatiotemporal distribution of seasonal ET _a during Maha season in Kirindi Oya and Menik Ganga.....	23
Figure 16: Spatiotemporal distribution of ET _a during the Yala season in the Kirindi Oya and Menik Ganga.	24
Figure 17: Frequency of water deficits in irrigated areas during the Maha season each year in Mi Oya (top basin) and Deduru Oya (bottom basin).....	25
Figure 18: Frequency of water deficits in irrigated areas during the Yala season each year in Mi Oya (top basin) and Deduru Oya (bottom basin).	26
Figure 19: Frequency of water deficits in irrigated areas during the Maha season each year in Kirindi Oya (left basin) and Menik Ganga (right basin).....	27
Figure 20: Frequency of water deficits in irrigated areas during the Yala season each year in Kirindi Oya (left basin) and Menik Ganga (right basin).	27

Figure 21: AGBP (kg/ha) for the Maha Season in irrigated areas within the Mi Oya (top basin) and Deduru Oya (bottom basin).	29
Figure 22: AGBP (kg/ha) estimates for the Yala Season in the irrigated areas of the Mi Oya (top basin) and Deduru Oya (bottom basin).	30
Figure 23: AGBP (kg/ha) for the Maha season in irrigated areas of the Kirindi Oya and Menik Ganga.....	30
Figure 24: AGBP (kg/ha) for the Yala Season in the irrigated areas of the Kirindi Oya and Menik Ganga.	31

LIST OF TABLES

Table 1 : Average monthly cloud cover percentages for Landsat 8 images over the four basins.	11
Table 2: Number of partially clouded images used for each basin and each season.....	11
Table 3: Meteorological data inputs to the PySEBAL model.....	14
Table 4: Change in length of season (LOS) compared over pre-2010 and post-2010-time period and difference in LOS presented for each basin.....	21
Table 5: Mean AGBP in kg/ha for irrigated areas within each basin for the Maha season ...	28
Table 6: Mean AGBP in kg/ha for irrigated areas within each basin for the Yala season.....	28

LIST OF ABBREVIATIONS

ADB	Asian Development Bank
AGBP	Above Ground Biomass Production
CDZ	Cauvery Delta Zone
CWP	Crop Water Productivity
CWSI	Crop Water Stress Index
DOI	Department of Irrigation
DSS	Decision Support System
ET _a	Actual Evapotranspiration
FAO	Food and Agriculture Organization
GEE	Google Earth Engine
GLDAS	Global Land Data Assimilation System
HI	Harvest Index
IHE Delft	IHE Delft Institute for Water Education
IWMI	International Water Management Institute
IWPIP	Integrated Water Productivity Improvement Project
MIWRDM	Ministry of Irrigation and Water Resources and Disaster Management
MODIS	Moderate Resolution Imaging Spectroradiometer
NASA	National Aeronautics and Space Administration
NDVI	Normalized difference vegetation index
PySEBAL	Python implementation of SEBAL
RWD	Relative Water Deficit
SRTM	Shuttle Radar Topography Mission
TA	Technical Assistance
WP	Water Productivity

I. INTRODUCTION

1. The ADB is committed under its Water Operational Plan 2011-2020 to undertake expanded and enhanced analytical work to enable its developing member countries to secure deeper and sharper understanding of water issues and solutions. IHE Delft, in collaboration with IWMI and FAO, will support ADB in achieving this objective.
2. The activities proposed under the current study build on the work previously undertaken by IHE Delft and IWMI in cooperation with the Asian Development Bank (ADB) to assess crop water productivity and to assess water resource status in selected countries in Asia.
3. Through the current study, IHE Delft in partnership with its subcontracted partner, IWMI, will support (a) ADB's lending and non-lending assistance in the water sector, and (b) the design of irrigation projects at an early stage at selected candidate projects.
4. IHE Delft and IWMI aim to support ADB's lending and non-lending assistance in the water sector by creating (i) comprehensive, (ii) comprehensible, and (iii) accessible information on available water resources and their current uses in major river basins. IHE Delft and IWMI aim to support the design of, or investments in irrigation schemes at project start by (i) providing baseline data for parameters related to land and water productivity, and (ii) identifying suitable interventions.
5. Assistance is being provided to Projects in 7 countries. The nature of the support provided in each is determined through close consultation with ADB Project Officers, and tailored to the project requirements. In some locations, this may take the form of water accounting assessments to characterize water use and availability, while in others emphasis may be placed on water productivity (either crop or biomass water productivity), or on irrigation performance assessments, to target investments.
6. This document is the Final Report for the Sri Lanka case study, and as such it details the activities undertaken by IWMI to support the Integrated Water Productivity Improvement Project.

II. PROJECT BACKGROUND

7. In February 2018, the Ministry of Irrigation and Water Resources and Disaster Management (MIWRDM) approached the Asian Development Bank (ADB) with a project proposal to improve irrigated agriculture and water productivity and enhance resilience to climate change in the Uva and North Western Provinces of Sri Lanka. A transactional technical assistance (TRTA) from ADB's Technical Assistance Special Fund was subsequently allocated to MIWRDM for the project.
8. Referred to as the Integrated Water Productivity Improvement Project (IWPIP), the objective of the Project is to improve water management within selected river basins in Sri Lanka, and take up irrigation subprojects for investment incorporating the objectives of;

(i) improved management of water resources; (ii) modernization of irrigation infrastructure; and (iii) promotion of modern crop production and marketing systems.

9. The project focus is on river basins that are mostly located within the North Western and Uva provinces. These river basins straddle the dry and intermediate climatic zones and have large numbers of smallholder farmers cultivating under both medium to large and small irrigation systems, as well as rainfed conditions. They are identified as areas which are (i) vulnerable to climate change; (ii) requiring interventions in irrigation and water resources management to develop resilience to climate change; and (iii) not currently covered by ongoing or planned interventions.

10. Project preparation is being carried out over 48 months between April 2019 to March 2021 and involves several tasks including: (i) selection of basins and sub projects, (ii) preparation of river basin management plans, (iii) sub project feasibility studies, and (iv) detailed design of investments.

11. Following project inception, the TRTA team and the MIWRDM identified three priority river basins in three provinces: (i) Deduru Oya and Mi Oya in the North Western Province, and (ii) Kirindi Oya which straddles the Uva and Southern Province. As part of the TRTA, the International Water Management Institute (IWMI) was contracted by ADB to assist in the selection of river basins, and to support basin planning activities, as well as to provide information on water availability and land use mapping for three river basins, Deduru Oya, Mi Oya and Kirindi Oya.

12. The current study, reported here, builds further on this analysis undertaken by IWMI in support of the TRTA; outputs of the analysis are used in the activities detailed in this report.

III. SCOPE OF SERVICES

13. There are 25 basins that lie partially in North Western, Uva, and Southern Province. The total gross area of the basins is 37,000 km² which is 56% of the total area of Sri Lanka. The basins have an estimated irrigation area of 280,000 ha consisting of 150,000 large and medium schemes and about 130,000 ha of small schemes. Selection criteria for the priority river basins have been prepared by the TRTA, and 7 basins have been short listed; of these, 3 priority basins have been selected for investment (the Mi Oya, Deduru Oya, and Kirindi Oya); The priority river basins are estimated to incorporate investment sub projects for about 30% of the total investment.

14. During the implementation of this study a fourth basin (Menik Ganga which straddles the Uva and Southern Province) was also identified as a priority basin. Following this decision, it was incorporated into the analysis and is also presented here.

15. Through discussions with ADB, IWMI and IHE Delft, it was agreed that the ADB program to support Water Accounting in River Basins and Water Productivity in Irrigation Schemes would be used to (i) support the selection and planning of the follow-on river basins, and (ii) inform the selection of sub projects for investment. IWMI has agreed to

undertake a remote sensing-based assessment to provide the information needed for this purpose.

16. The first will be achieved through an assessment of trends and changes in crop phenology and vegetation growth in irrigated areas using the Normalized Difference Vegetation Index (NDVI) across the 25 river basins over a 20-year period using moderate spatial resolution (250m) remote sensing data from the MODIS satellite; and the second through the use of higher spatial resolution (30m) Landsat data and a spatial and temporal assessment of two parameters related to water deficits and crop growth.

17. In terms of the first parameter, a “Relative Water Deficit” indicator was agreed upon to identify spatial variations in water availability as a proxy for potential issues in water delivery during the irrigation seasons. ADB have requested that this indicator to be calculated as the difference between reference ET (i.e. water unlimited ET during crop development), and actual ET (ET_a). For the second parameter the Above Ground Biomass Production (AGBP) will be used as a proxy indicator for crop growth.

18. IHE Delft and IWMI have proposed to use the pySEBAL approach (detailed in IHE Delft and IWMI, 2020) for analyses at the irrigation command scale to derive the data on AGBP and ET_a; this approach uses satellite images and weather data as inputs. PySEBAL processes the surface energy balance and plant growth at landscape level with a grid of 30 m independent of crop type information. The ET_a and AGBP can be estimated without any a priori information on the type of crop and type of soil. This approach, and the pySEBAL tool in particular, have been developed through, and widely used in other similar studies funded by ADB and implemented by IHE Delft and IWMI.

19. During subsequent discussions IWMI has agreed to contribute to additional activities as follows:

- a. Selection of tanks and tank cascades: investigate potential approaches to link the location of small tank cascades to the water deficit outputs;
- b. Support to WEAP modelling for large and medium sized tanks: use of the water deficit and ET_a data to compare and validate the seasonal deficits output from the model;
- c. Support to a TA on groundwater: use of the water deficit data to select locations for solar powered piezometers within the priority river basins.

This additional analysis is presented in a separate report (Report B).

IV. VEGETATION GROWTH AND WATER DEFICIT ASSESSMENT

A. Background: Site Description

20. Sri Lanka is a tropical island of mild climate without extremes. Most of the country's land area consists of tropical plantation. In the past century the pattern of land use has changed with forest cover reduced from 70% in 1901 to 24% in 1996. Removal of forests for plantation agriculture was the greatest cause of land cover changes. The major agricultural crops are paddy rice, tea, rubber and coconut. Rice is usually irrigated, although some rain-fed rice cultivation is practiced. The rainfall distribution in Sri Lanka is influenced by monsoons, the intertropical convergence zone (ITCZ), convection, orography, easterly waves and cyclonic wind circulations. Paddy rice is the third largest consumer of fresh water resources in Sri Lanka (Bastiaanssen and Chandrapala, 2003).

21. Within Sri Lanka, a typical irrigation system consists of a series of catchments each with a tank (or reservoir) at the head, from which water is diverted for irrigation. The return flow from the irrigated land forms the inflow for the tank downstream. The tank cascade systems have multiple uses including domestic supply and irrigation as well as sustaining natural vegetation. There is wide variation in the size of cascades, ranging from a few small tanks to the large cascades which may involve multiple large and small tanks and sometimes inter basin transfers. Individual irrigation schemes within the cascades are a wide mix of sizes and characteristics.

22. The irrigated paddy farming is typically supplied with water through the extensive number of small and medium tanks that capture monsoonal rains. There are approximately 533 major irrigation schemes under the Department of Irrigation serving an extent of about 340,000 ha; in addition, there are nearly 25,000 minor irrigation schemes which fall under the Department of Agrarian Services, serving an area of around 162,000 ha. These lands together with the Mahaweli project which was commenced with the target of providing irrigation facilities to 265,000 ha of new land and 100,000 ha of existing agricultural lands indicate the magnitude of irrigated agriculture in the country. The total land under paddy cultivation in 2010 was 1,065,000 ha, which is approximately 16% of the total area of Sri Lanka (Wijesekera, 2015).

23. This study calculates and analyses vegetation growth across the 25 river basins (Figure 1) over a 20 year period, as well as the water deficits and AGBP within the four priority river basins (Deduru Oya, Mi Oya, Kirindi Oya and Menik Ganga; Figure 1). Two of the four priority basins are located in Southeast of the Island (Kirindi Oya and Menik Ganga) and the other two are located in Northwest of the Island (Mi Oya and Deduru Oya).

24. The Kirindi Oya basin has a catchment area of 120,300 ha and receives an average annual rainfall of 1455 mm. The Menik Ganga basin has a catchment area of 127,200 ha and receives average rainfall of 1576 mm. Both the Southeast basins receive the majority of the annual rainfall during the northeast monsoon period from November to January and remain mostly dry from June to September. The topography of the basins varies from hilly regions in the north and coastal flat plains in the south. Forests are the dominant land cover type in these basins, while rice and sugarcane are the major crops grown. The higher crop water requirement of rice, sugarcane and the climatic condition of

these basins gives rise to water deficit issues in the farming systems (Abeysingha et. al., 2017).

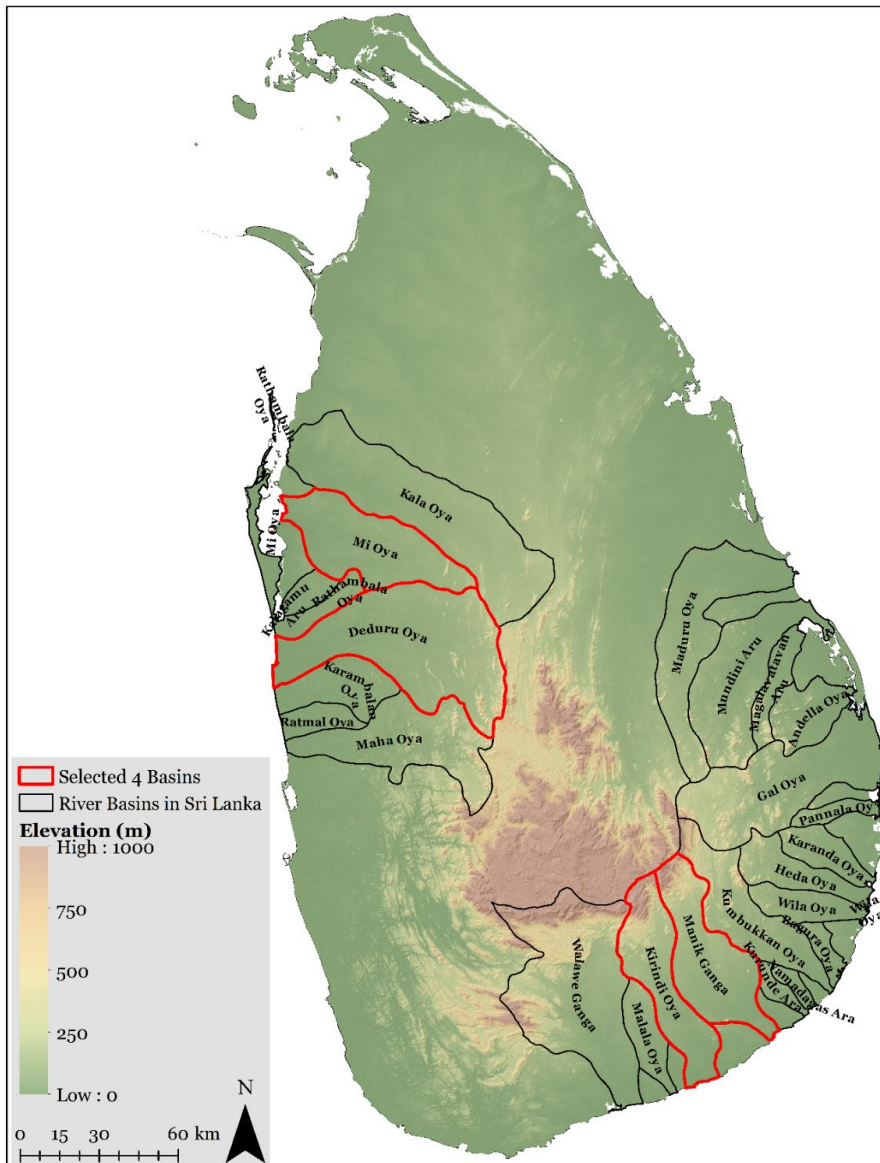


Figure 1: Topography of Sri Lanka along with the boundaries of the 25 basins to be analysed, with the four which have been identified as priorities for investment highlighted in red (Source: SRTM and IWMI estimates).

25. In the Northwest, the Mi Oya basin has a catchment area of 102,400 ha and it receives 1250 mm average rainfall annually, while the Deduru Oya basin has a catchment area of 262,300 ha and receives average annual rainfall of 1600 mm. The first half of the year is the dry season in these basins. The topography of the basins varies from hilly regions on eastern boundary (elevation 700 m), to coastal flat plains on the western. More than 90% of the land in these basins is devoted to agriculture, consisting of mainly coconut and paddy rice. The basins contain a number of small and large tanks. There are also a

large number of private lift irrigation schemes, notably in the downstream reach of the water channels (Samarasinghe et. al, 2000; Wickramaarachchi, 2004).

26. Paddy (rice) is the major crop cultivated in the irrigated areas in Sri Lanka. Paddy is cultivated during two seasons; the Yala season (April to August), and the Maha season (mid-October to mid-March) As most of the rainfall is received during the second half of the year, the Maha is known as the wet season (and is the primary cropping season), and the Yala is the dry season crop.

27. The distribution of average monthly rainfall and potential evapotranspiration for the 25 basins over 2014-2018 is presented in Figure 2. An average rainfall of 2,200 mm is received per year, with potential evapotranspiration accounting for up to 90% of the annual rainfall. The rainfall has a bimodal distribution; The Maha season received around 55-60% of annual rainfall and October, November and December are typically the wettest months. Since the evaporative demand (ETp) is lower than the rainfall received during the Maha season, a positive water balance indicates greater water availability.

28. The Yala season receives up to 40-45% of the annual rainfall, and April, May and June are the wettest months in the season. As the evaporative demand is higher than during the Maha season months, a negative water balance leads to lower water availability for crop growth during the season.

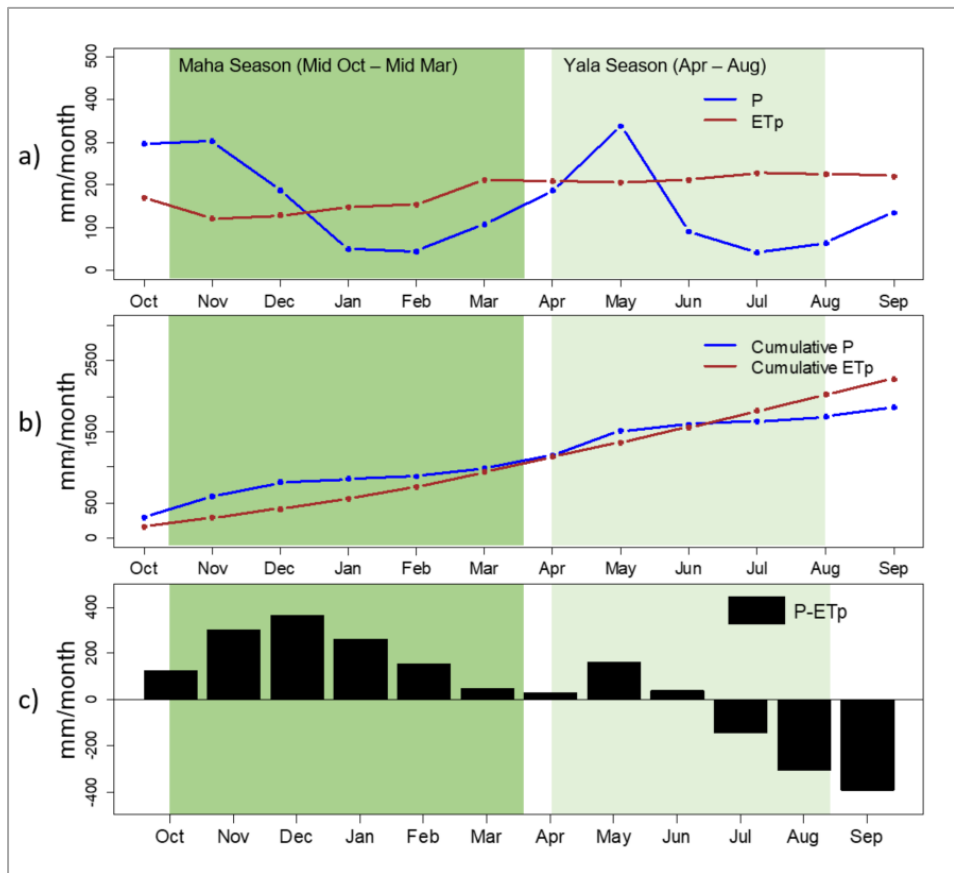


Figure 2. Distribution of average monthly rainfall (P) and potential evapotranspiration (ETp) for the 25 basins during 2014-2018; a) absolute monthly estimates of P and ETp; b) cumulative estimates of P and ETp, and, c) the water balance (P-ETp).

B. Summary of the approach

1. Analysis of irrigated crop phenology

29. Remote sensing data has been used to characterize vegetation growth and phenology within the irrigated areas over the 25 river basins (Figure 1). The objective of this analysis is to identify trends and changes using the Normalized Difference Vegetation Index (NDVI) over the past two decades, to assist in prioritizing basins for investment (i.e. to assist in identifying where agricultural production may have remained static or decreased). The steps followed in the analysis are summarized in the flow chart in Figure 3.

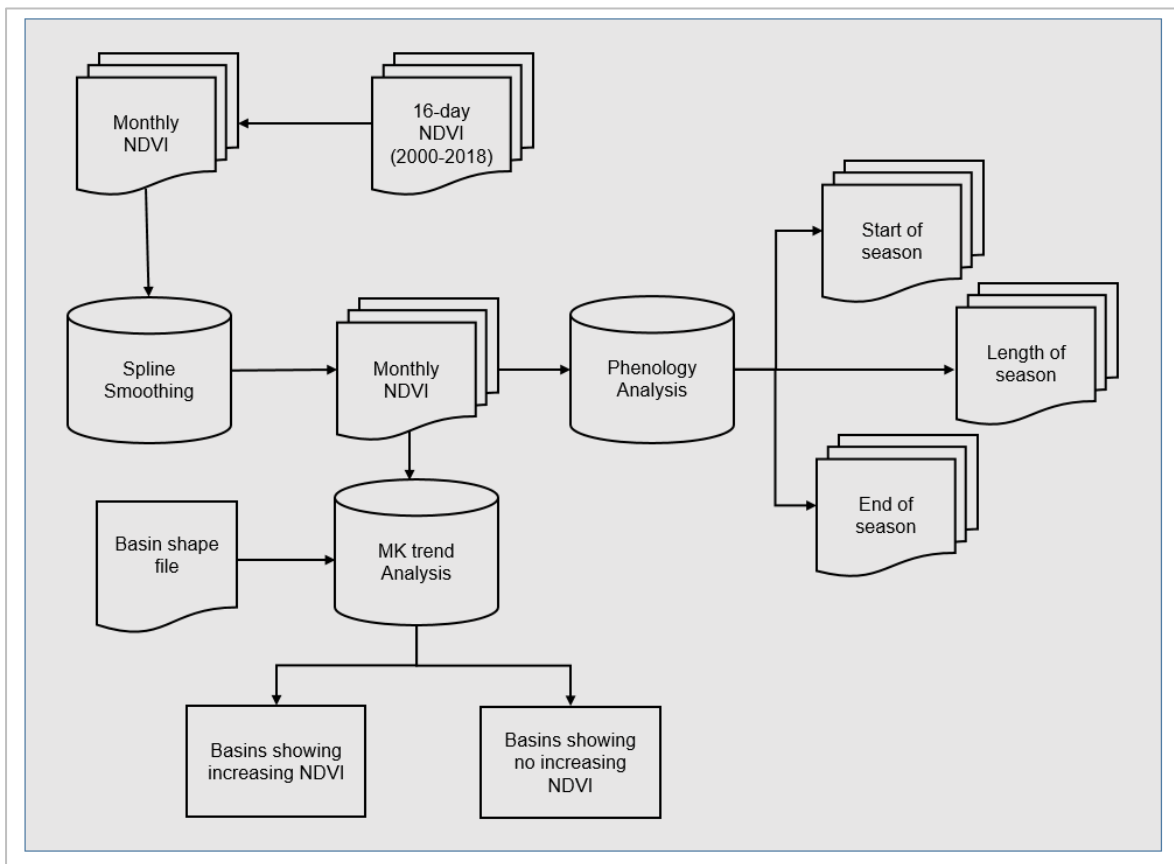


Figure 3. A flowchart showing the describing the processing steps for the phenology analysis for the 25 river basins.

30. Given the areal extent of the analysis and the time period of interest, 16-day MODIS 250 m NDVI data have been used for the period 2000–2018. Prior to analysis, the 16-day composite data have been interpolated to daily intervals using a spline smoothing function. These were subsequently aggregated to monthly and annual datasets.

31. The only available land cover map for Sri Lanka which details irrigated areas (IWMI, 2013; Figure 3) was used to select MODIS NDVI pixels corresponding to irrigated croplands within each basin.

32. MODIS NDVI is used to study the crop phenology. Phenology is the study of periodic events in the crop life cycle such as the start of the season (SOS), the end of the season (EOS), and the length of the growing season (LOS) and how these events are influenced by seasonal and inter-annual variations in climate (such as droughts) or agronomic factors (such as irrigation). Analysis of phenology metrics over the irrigated areas can provide several insights into crop performance.

33. Cropland phenology analysis was performed to characterize the cropping seasons, including start, end, and length of the growing season for each pixel over the 2000-2018 period. Analysis was performed using the R programming language using functions available through the greenbrown package (Forkel and Wutzler, 2015).

34. The mean NDVI for each of the basins was extracted and used as input to the phenology analysis. A spline function was applied to smooth the data and to improve analysis of the seasonal variations present in the NDVI data.

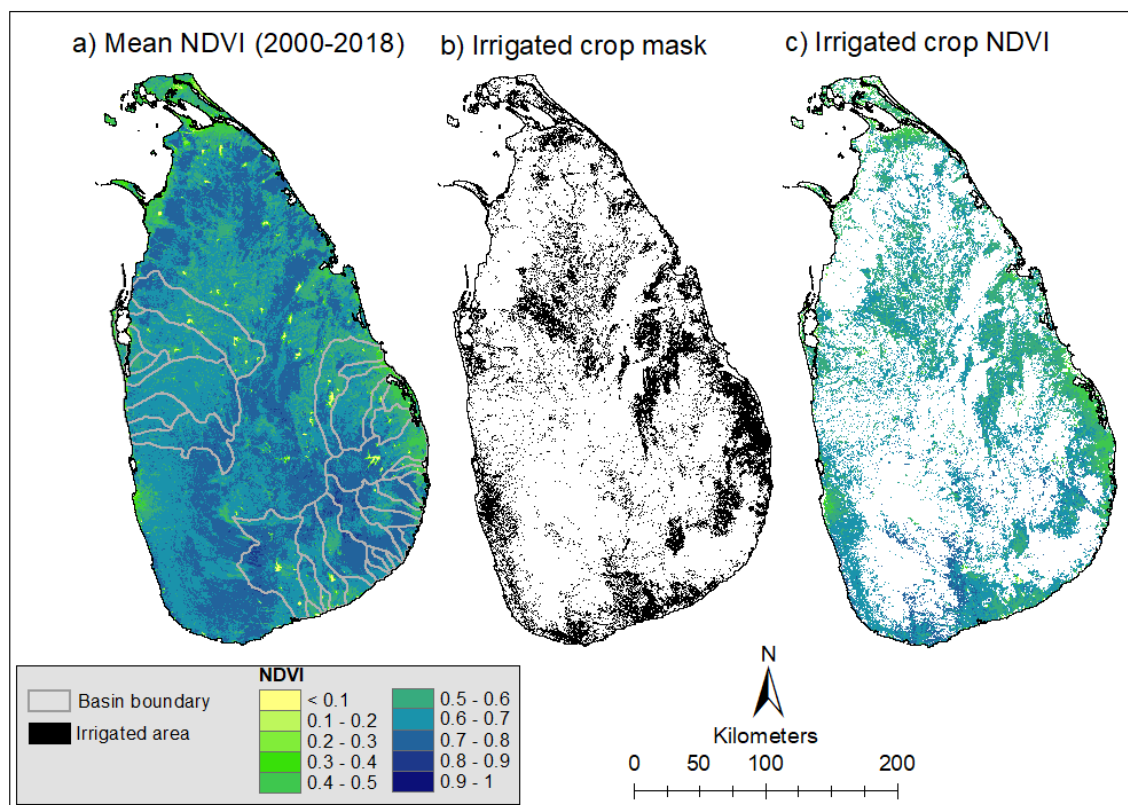


Figure 4: Data used for the phenology analysis; a) Mean NDVI over 2000-2018 with basin boundaries; b) Irrigated crop map (IWMI, 2013) and c) Mean NDVI for the irrigated areas.

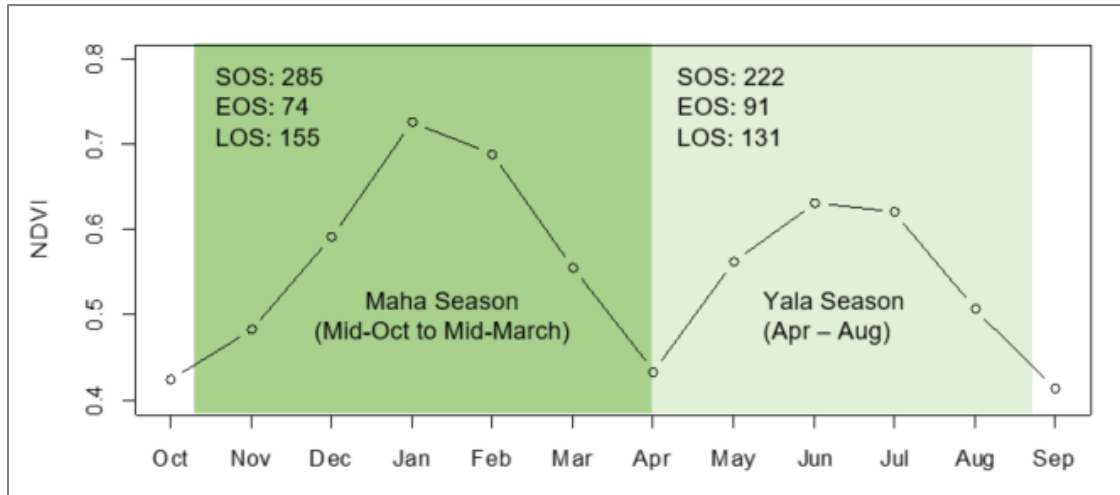


Figure 5: Illustration of phenology parameters (start of season, SOS; end of season, EOS and length of season (LOS)) for irrigated rice fields in Sri Lanka derived from the time-series of NDVI data. SOS, EOS and LOS are shown as day of the year.

35. For the purpose of this analysis, several phenology related parameters were obtained using the ‘greenbrown’ package in R using the NDVI time series as input. Three key indicators (start of season – SOS, end of season – EOS, and length of season – LOS) were derived to improve understanding of any potential changes in the cropping patterns across the basins.

36. An analysis of trends in the mean NDVI was performed for the irrigated areas over the 2000-2018 time period. A Mann-Kendall trend analysis was conducted on the monthly NDVI estimates to identify the presence of any long-term trends.

2. Water Deficit Analysis

37. Water Productivity (WP) is a performance indicator that can be used for monitoring, evaluating, and diagnosing agricultural water management practices; the concept is described in detail in the technical manual developed through this project (IHE Delft and IWMI, 2020).

38. WP focuses on the consumed water; the water productivity of agricultural activities can be quantified on the basis of crop yield harvested and net water consumed. Remote Sensing (RS) based assessment of WP focuses on actual evapotranspiration (ET_a) to estimate net water consumption. IHE Delft and IWMI, through discussions with ADB, have agreed to use the pySEBAL tool for this purpose.

39. pySEBAL is a library of python codes used to implement the Surface Energy Balance Model (SEBAL) from spatial data including spectral reflectances, climatic parameters, and altitude as inputs to estimate the surface energy balance components (Bastiaanssen et al., 1998a, 1998b). The outputs include parameters related to the energy balance, vegetation and biomass, the ET, and WP.

C. pySEBAL Implementation

40. SEBAL is a single-source model that uses visible, near-infrared and thermal infrared data collected mainly by sensors on board earth observation satellites (Bastiaanssen, 2000). SEBAL has the advantage over conventional methods of estimating ET from crop coefficient curves or vegetation indices in that crop development stages do not need to be known, nor do specific crop types.

1. Data inputs

41. A full specification of data requirements for the PySEBAL model are detailed in IHE-Delft and IWMI (2020). Only data which are specific to the current analysis are discussed further.

42. Spectral radiances in the visible, infra-red and thermal range of the electromagnetic spectrum are the main input to the SEBAL model. Data from the Landsat satellites are typically used as inputs to pySEBAL; the high spatial resolution (30m) of the data provides sufficient detail to characterize the spatial patterns of biomass production and water deficits across the command area, and the revisit time of 16 days can, under cloud free conditions, provide sufficient coverage of an irrigation season.

43. Four Landsat images from three consecutive paths (see Figure 1) and three rows are needed to cover the entire area of the four basins: Mi Oya, Deduru Oya, Kirindi Oya and Menik Ganga. The data are available for download at no cost from the USGS Earth Explorer website (<https://earthexplorer.usgs.gov/>).

44. A total of 337 Landsat 8 images were downloaded and processed for a five-year period (2014-2018; see Annex A for image details and Table 1 for summary). Images with a threshold of less than 75% cloud cover on land were downloaded and further interpreted to ensure the images with low cloud cover had usable data over the selected basins.

45. Acquiring cloud free images during each month with only a single satellite overpass in every 16 days is a challenge (Landsat 7 data are not available for Sri Lanka). Therefore, only Landsat 8 are available for the analysis, and consequently, it was necessary to include images with higher than the usually acceptable cloud cover amounts. A list of the selected images for this study with the information on cloud cover and the image viewer link is provided in Annex A. In some of the months (May, June and July in 2015 and 2016) no usable images were available during the growing season due to cloud cover.

46. Cloud cover over the period of analysis is summarized in Figure 6 for the Maha and Yala seasons over the period 2014-2018. Table 2 presents the number of images available over each growing season for the four priority basins. On average, there are 15 to 17 images available for analysis each season, except for the Yala season of 2015 and 2016, where 10 or less images were available in all basins. It is important to note that none of the images were cloud free with cloud cover of 30% typically observed for each season in every basin.

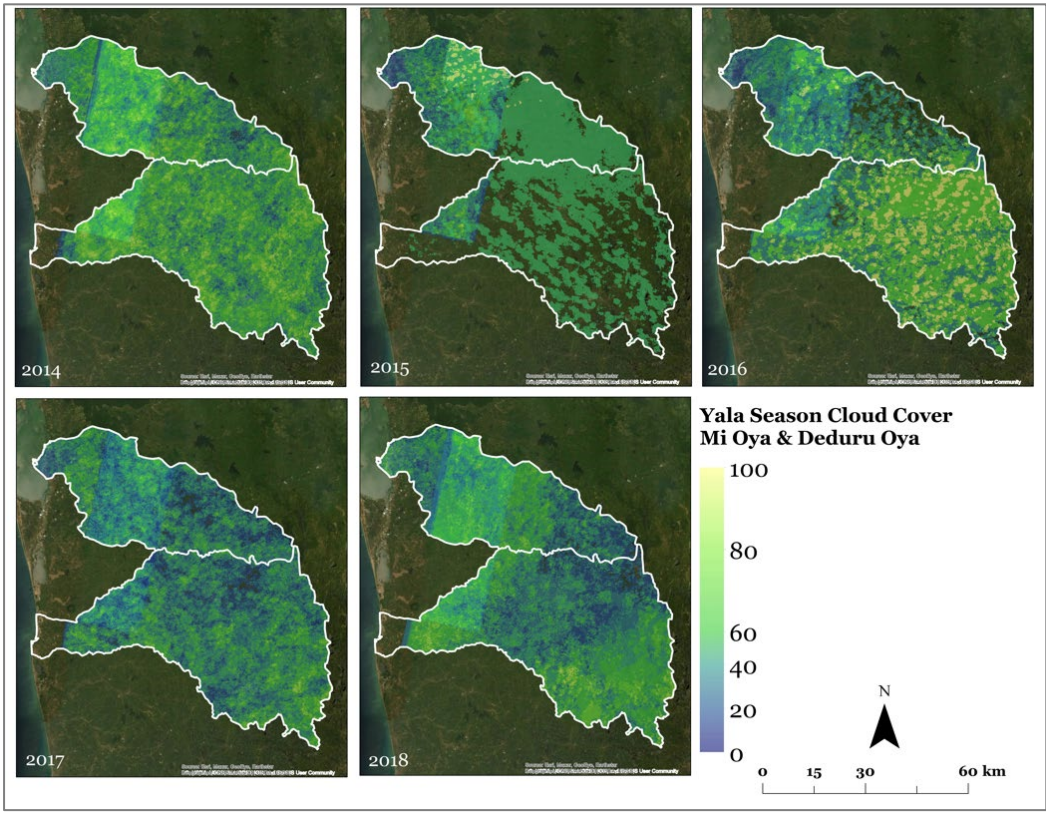
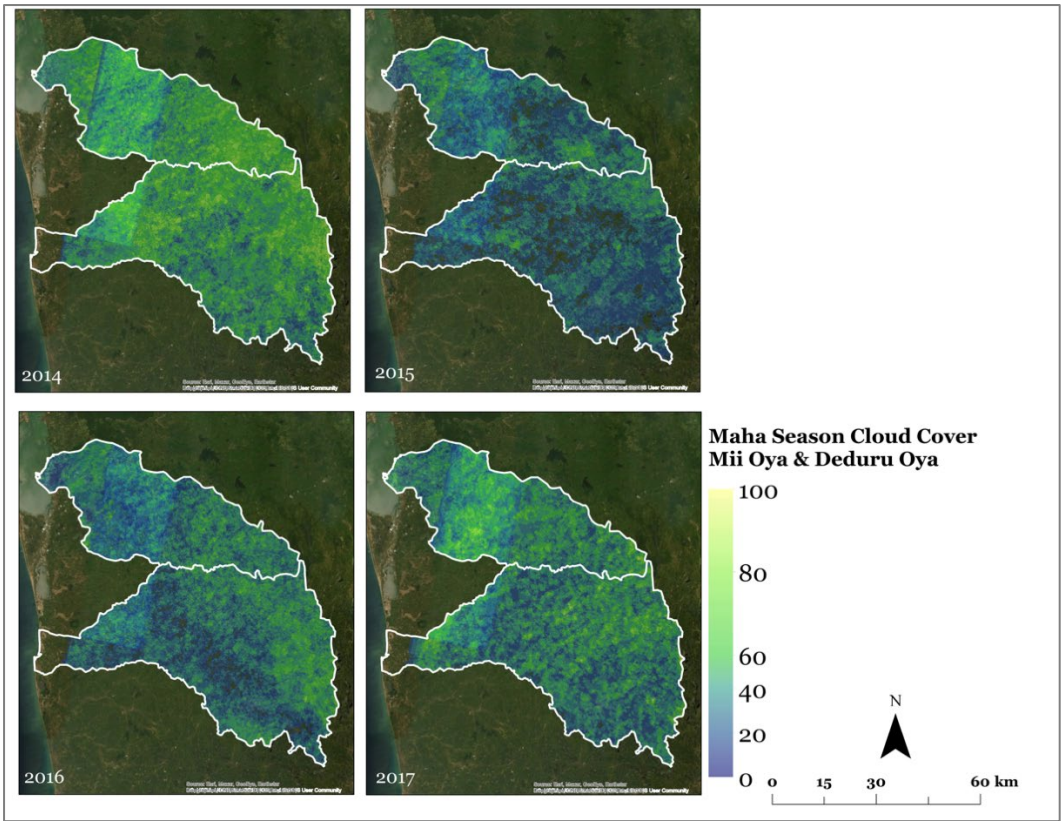
47.

Table 1 : Average monthly cloud cover percentages for Landsat 8 images over the four basins.

	2014	2015	2016	2017	2018
Jan	39.34	28.67	24.30	22.20	63.59
Feb	14.85	49.81	19.91	71.30	25.61
Mar	19.48	46.64	15.91	39.28	19.78
Apr	28.01	20.88	39.24	15.83	45.14
May	36.12	72.02	38.91	66.62	48.13
Jun	46.80	73.99	73.65	41.32	52.60
Jul	46.05	44.72	46.29	39.95	68.78
Aug	84.42	47.22	50.98	42.92	48.03
Sep	65.22	55.83	48.90	70.97	32.32
Oct	50.21	52.71	34.28	47.66	53.45
Nov	90.41	56.56	52.73	56.83	26.68
Dec	83.04	69.58	40.98	27.27	25.52

Table 2: Number of partially clouded images used for each basin and each season.

Maha Season	Mi Oya	Deduru Oya	Kirindi Oya	Menik Ganga
2014	15	15	16	16
2015	16	16	17	17
2016	17	17	17	17
2017	18	18	17	17
Yala Season				
2014	18	18	15	15
2015	9	9	10	10
2016	9	9	8	8
2017	18	18	15	15
2018	17	17	15	15



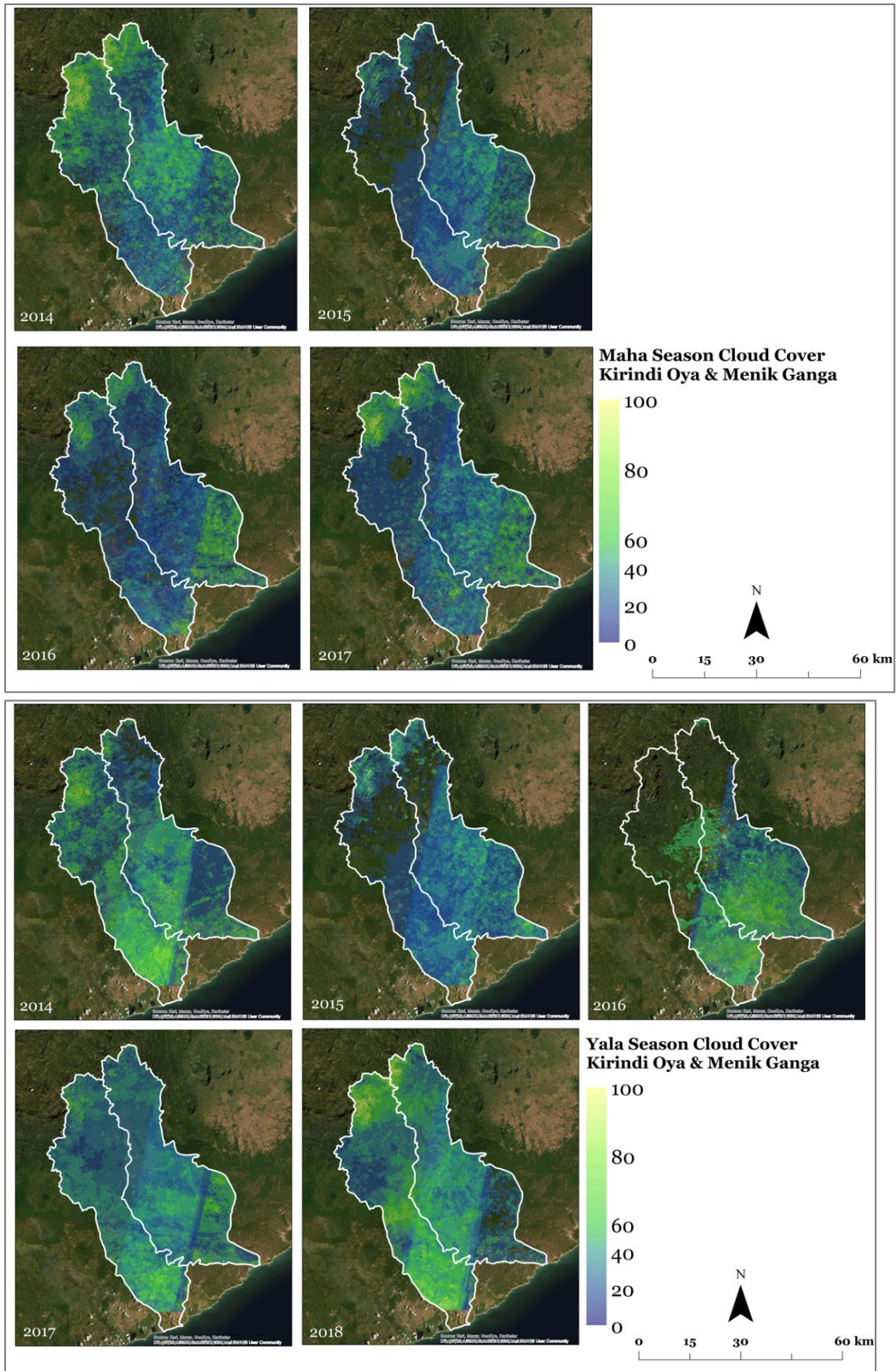


Figure 6: Cloud cover percentage during Maha and Yala growing seasons for the two northern (Mi Oya and Deduru Oya), and the two southern (Kirindi Oya and Menik Ganga) river basins

48. A time-series of meteorological parameters are required to implement the pySEBAL model; these are needed to calculate the soil water balance and Penman Monteith Standard Reference Evapotranspiration (see IHE Delft and IWMI (2020) for full details).

49. Instantaneous (hourly) and daily average data from the NASA Global Land Data Assimilation System (GLDAS v2.1; <https://ldas.gsfc.nasa.gov/gldas>) were acquired for the command areas and used as input to the pySEBAL model. GLDAS is an assimilated global data product from satellite and ground-based observations, with data available at 0.25-degree spatial resolution and at 3 hourly intervals. The parameters used are listed in Table 3.

Table 3: Meteorological data inputs to the PySEBAL model

Parameter	Symbols	Unit
Downward shortwave radiation	SWdown	W/m ²
Wind speed	Ws	m/s
Air temperature	Tair	°C
Pressure	P	Mb
Relative humidity	Rh	%

50. A Land use/land cover (LULC) map or a map depicting the location of irrigated areas, or boundaries of the irrigation systems, is needed to ensure that the analysis is limited to the relevant areas. As no recent or high resolution LULC map was available for the study area, a previously generated irrigated area map (IWMI 2013) was used to identify the areas of irrigated single, double and continuous/three cropping regions (Figure 7) for further analysis.

51. According to this map the greatest areas of double cropped land are located in the Kirindi Oya Ganga (left basin, left panel of Figure 7), downstream of the large reservoir in the south of the basin. The Menik Ganga basin (right hand basin, left panel) has mostly single cropped land with some rain fed areas. Similarly, in the Mi Oya basin (top basin, right panel of Figure 7) irrigated single cropping is the dominant irrigated system, and rain fed areas are also extensive. The Deduru Oya basin (lower basin, right panel) has more irrigated area under double cropping situated closer to the water channels.

52. Following the collection and preparation of the various input datasets, the pySEBAL model was implemented according to the steps shown in Figure 8. The acquired Landsat 8 data was pre-processed to create cloud masked Top of Atmosphere (TOA) reflectance. The pre-processing included conversion from Digital Number (DN) to TOA reflectance, cloud removal using the Quality Assessment (QA) band provided along with the data, and mosaicking the same image path tiles. These pre-processing steps (Steps 1 and 2, Figure 8) are performed inside pySEBAL.

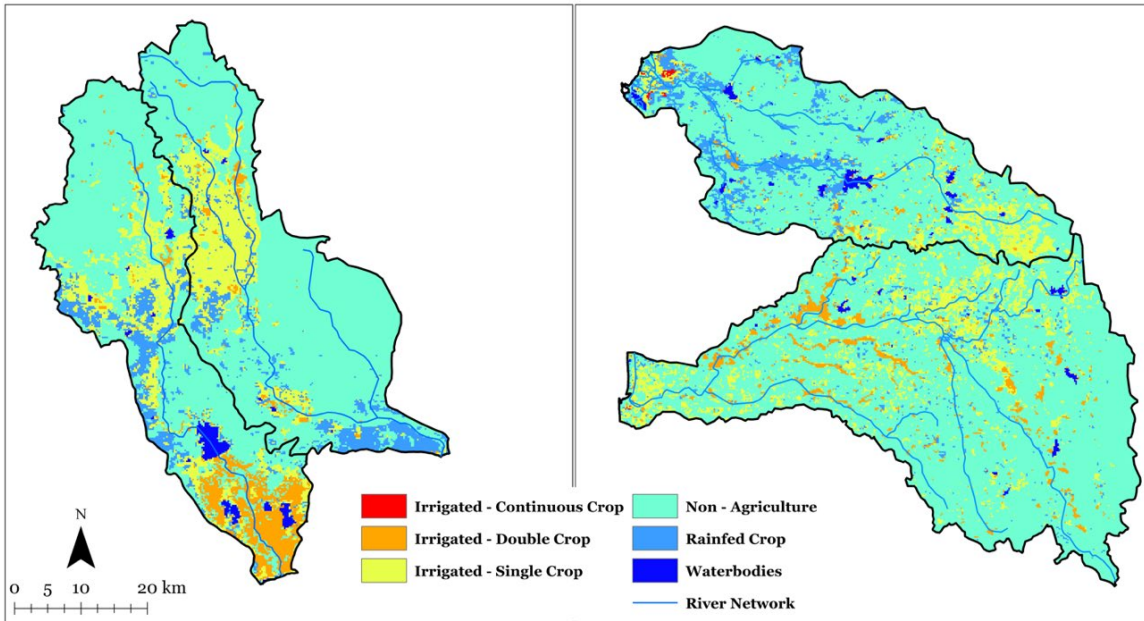


Figure 7: Map of irrigated areas for the four basins (Left panel Kirindi Oya and Menik Ganga, right panel Mi Oya and Deduru Oya; Source: IWMI 2013).

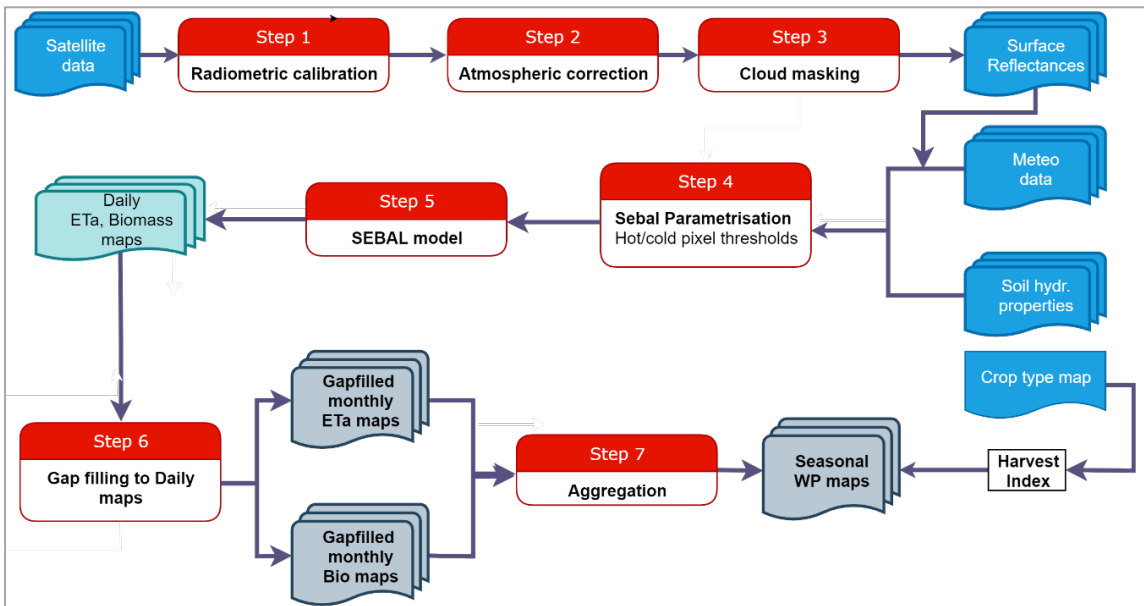


Figure 8: The pySEBAL methodological framework (Source: IHE Delft and IWMI, 2020).

2. Cloud masking and gap filling

53. The pySEBAL approach is dependent on the availability of cloud free satellite images of the land surface during the period of interest for the selected project sites. While the Landsat satellites data archive is one of the most useful data products to monitor the Earth’s surface at a high spatial resolution, given the temporal coverage of 16-day, the degree and extent of cloud coverage is always a challenge and will vary from region to

region. Due to the proximity to the coast and the monsoon climate, the irrigated areas in the four basins show a high degree of cloud cover throughout the year.

54. The images selected for analysis still contain cloud cover of varying amounts (see Table 1, Figure 6). In the standard pySEBAL implementation, areas covered by clouds are identified, masked out and subsequently filled using a linear interpolation algorithm. While this is a suitable approach for land cover classes which are relatively static between consecutive image dates (e.g. forests), using a linear interpolation algorithm can result in inaccurate estimation of ET_a. This is due to the fact that the cloud-free image acquisition dates could be 32 days apart, or more in Sri Lanka where cloud cover is common during the cropping season. Moreover, some rain events may occur in between satellite images, the effects of which are not recorded in a subsequent image, and therefore those evaporation amounts are not fully accounted for. Hence, linear interpolation does not suitably capture the effect of vegetation growth following the last image and does not reflect for any antecedent soil moisture (Irmak et al., 2012).

55. We therefore applied an approach to the crop coefficient (“kc”) image obtained from pySEBAL; the approach uses the pySEBAL cloud mask image, and adds an extra processing step. The gaps in the kc image following the cloud masking are filled using a linear, time-weighted interpolation of the kc values from the previous image and the nearest following satellite image date which has a valid kc estimate, adjusted for vegetation development. In gap filling procedure, the interpolated values for the clouded and cloud-shadowed areas are adjusted for differences in residual soil moisture between the image dates which occur as a result of heterogeneities in precipitation (for example localized showers) in inverse proportion to the Normalised Difference Vegetation Index (NDVI), and by adding an interpolated ‘basal’ kc from the previous and following satellite image dates. The procedure is explained in detail in Irmak et. al., (2012).

3. Water Deficits and Biomass Production

56. The ET deficit is an essential performance parameter that is output from the pySEBAL approach. The ET deficit is calculated as the ratio of the potential evapotranspiration (ET_{max}) which represents the water unlimited ET during crop development, and the actual (measured ET; ET_a). The ET deficit is a direct expression for any water shortage the crop is experiencing on a pixel by pixel basis, and it can help to assess (without any further information on canal flows) whether the crop has sufficient moisture in the root zone. This information is useful in understanding and interpreting irrigation performance across a command area.

57. Through discussions with ADB, the ET deficit was normalised (i.e. so that the values varied between 0 and 1, where 0 indicates no deficit and 1 indicates high deficit) and referred to as a “Relative Water Deficit” (RWD). The RWD was calculated according to Equation 1 where ET_a/ET_{max} is the ratio of the actual ET (based on the satellite images and derived through the pySEBAL model; see IHE Delft and IWMI 2020 for full details) to the maximum evapotranspiration).

$$RWD = \left(1 - \left(\frac{ETa}{ETmax}\right)\right)$$

Equation 1

58. The Relative Water deficit (RWD) index can be used to identify the areas that suffer the most from lack of irrigation water availability and access, as it broadly shows where irrigation water has been insufficient to meet the crop water requirement (Steduto et al., 2012); assessment of the RWD can provide insights into deficit conditions across the command area for a particular crop (in this case paddy rice), over a particular season (in this case the Maha and the Yala seasons). The RWD often correlates with other biophysical parameters such as biomass and ETa. For example, regions with high RWD translate to low crop biomass production, which in turn gives an indication of the areas where there are yield losses due to limited water supply.

59. The second parameter calculated from the remote sensing data is the Above Ground Biomass Production (AGBP). The calculation of AGBP is primarily based on the relationship between the absorbed light and carbon assimilation by the plant. This relationship in most plants is relatively constant. This ratio, termed light use efficiency, is used to convert remote sensing-based estimations of light absorption to gross primary productivity (GPP). Consequently, the net primary productivity (NPP) is calculated after subtraction of carbon lost to autotrophic respiration (AR) from the GPP. NPP is then used to estimate dry biomass production using a conversion factor from organic carbon to dry organic biomass. The AGBP is an output from the pySEBAL approach, and full details of the algorithms and inputs used to calculate this and related parameters can be found in IHE Delft and IWMI (2020).

D. Presentation of Results

1. Analysis of irrigated crop phenology

60. The objective of the 25 basin phenology analysis was to help in selecting additional/follow on basins for investment. The analysis of the NDVI time series for the irrigated pixels across the 25 basins broadly demonstrates either a unimodal, or a bimodal phenology curve, corresponding to one or two irrigation seasons, the Yala (April to August) and/or the Maha (October to March) respectively. A high year-to-year variability in the monthly NDVI estimates and cropping seasonality is also evident, which indicates that vegetation growth varies from year to year.

61. The NDVI phenology curves for most of the basins (and for most of the years) demonstrate a clear distinction between both the seasons following the example given in Figure 5. However, some basins show exceptions. For example, the time-series of the NDVI from an irrigated field in the Mi Oya basin (Figure 9) lacks a clear separation between the end of the Maha and the beginning of the Yala seasons (which would be identified through the decrease in NDVI to the season start level, enabling the end of the season to be detected) is absent, as the start of the Yala season immediately follows the end of the Maha season. In these cases, the inter-season NDVI between Maha–Yala is only indicated by a small dip in the curve.

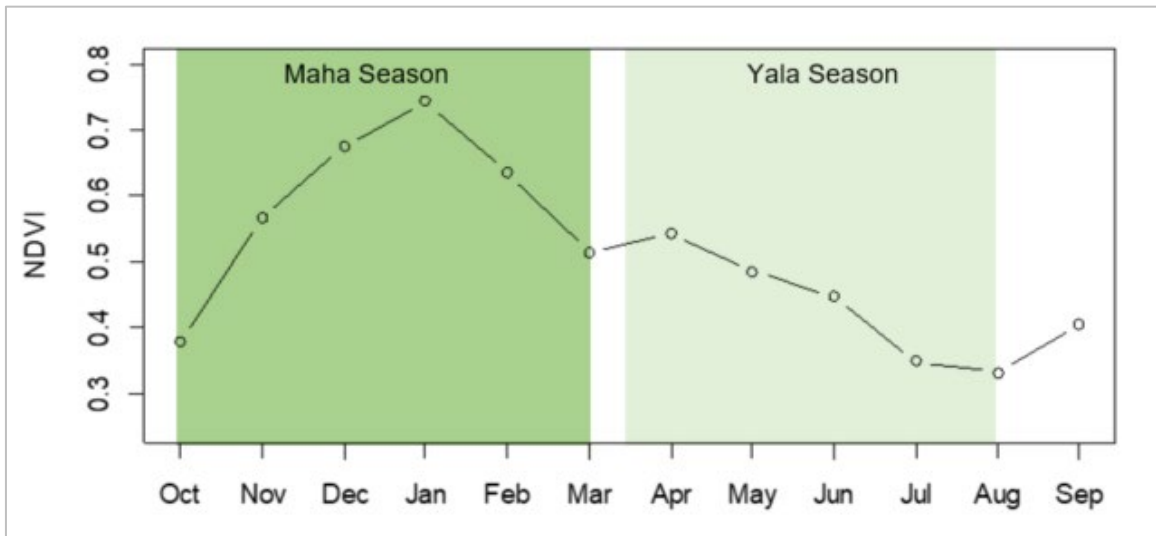


Figure 9: Mean NDVI time-series for the Mi Oya basin (2000-2018) showing the Maha and Yala cropping seasons separated by an insignificant change in NDVI profile, thus representing an unimodal curve.

62. In comparison, a clear distinction can be seen between the end of the Yala season and the beginning of the subsequent Maha season as NDVI drops down to values lower than 0.3. Similar trends can be seen in basins such as Maha Oya, Katupila Ara, Malala Oya, Manik Ganga, Kirindi Oya, Kalagaam Aru, Deduru Oya, Walawe Ganga, Kurunde Ara and Karambalan Oya (see Figure 1 for basin locations).

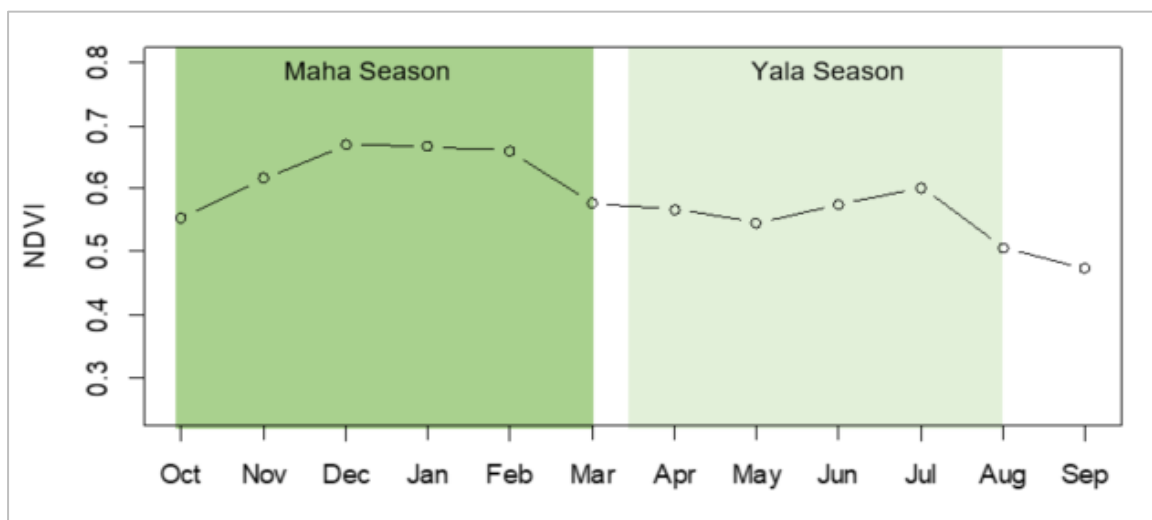


Figure 10. Mean NDVI profile in Karanda Oya Basin showing absence of distinct seasonal changes in NDVI.

63. Of the 25 basins, some basins, such as the Karanda Oya (Figure 10) do not show distinct seasonal changes in the NDVI, where end of the season NDVI does not decrease below 0.5. This may be due to the presence of continuous tree cover around the irrigated

areas as shown in Figure 11 below. This results in the signal for the irrigated areas being “diluted” with the relatively constant high NDVI from the surrounding forest.

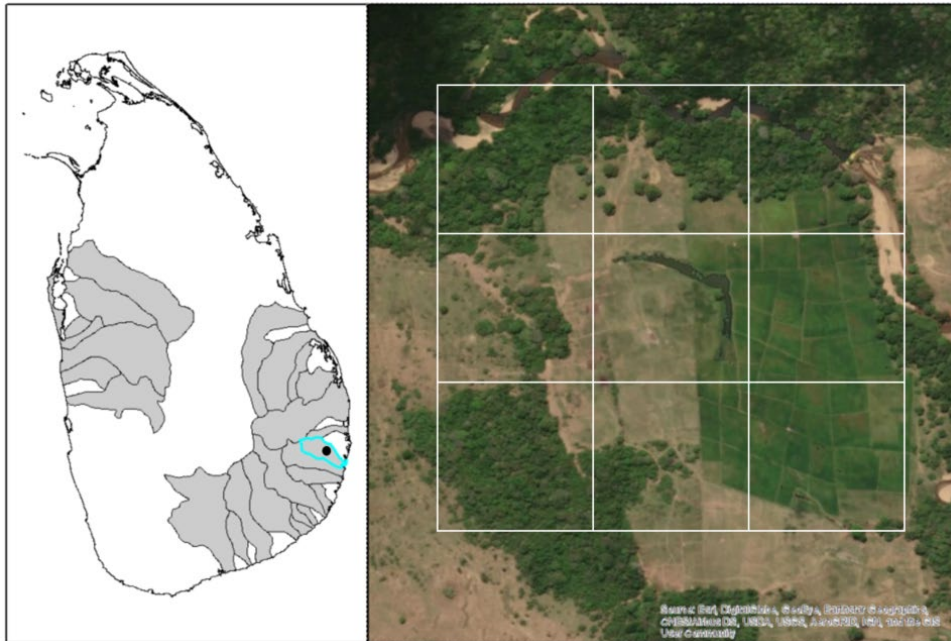


Figure 11. Presence of tree cover in and around irrigated fields in the Karanda Oya basin. The grid represents the 250 m irrigated pixels. The location of Karanda Oya basin is shown in the left panel in cyan; the black dot indicates the location of the grids.

64. To understand the trends in the irrigated crop phenology parameters, we analyzed the start of the season (SOS), end of the season (EOS), and length of the season (LOS) parameters for all of the 25 basins. Figure 12 shows the SOS, EOS and LOS presented as the deviation from the long-term mean for the Kirindi Oya basin. The results indicate that the SOS dates show less year-to-year variability, while the EOS and LOS both showed higher variability, suggesting that while the start of the season is relatively constant over the 18-year time period, the length of the growing season and thus the end of the season are much more variable.

65. The LOS was found to be around 20 days shorter prior to 2010 compared to the long-term mean. During this decade (2000-2010), the cropping season ended earlier. Since 2010, the data show that the irrigation season ended later, resulting in an extension to the length of the growing season by approximately a month during the more recent years. Other basins showed a similar trend in the LOS parameter.

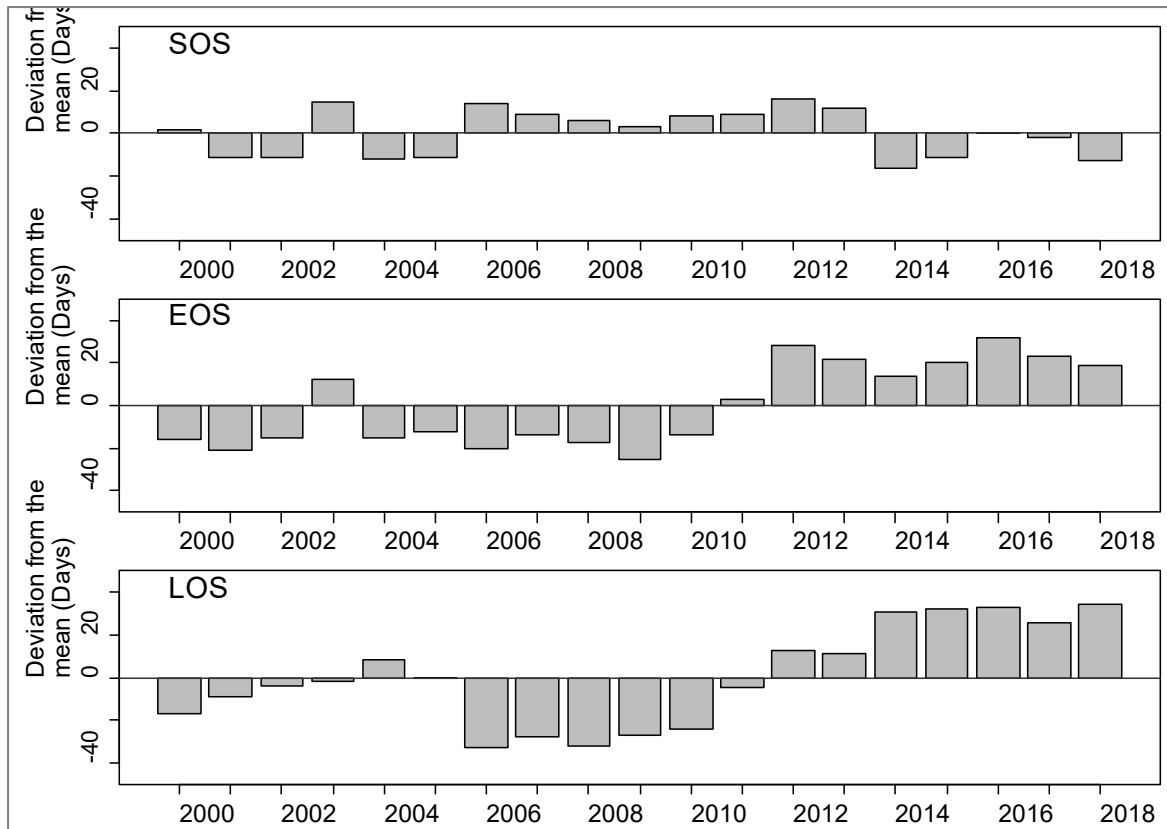


Figure 12: Deviation from the mean for each of the crop phenology parameters analysed: Start of season (SOS), End of season (EOS) and Length of season (LOS) for the cropping seasons (Maha + Yala) in the Kirindi Oya basin, Sri Lanka over the period 2000 – 2018.

66. A comparison of the mean LOS for the irrigation seasons during more recent years (2010 onwards) against the pre-2010 mean, shows that since the year 2010 the LOS has extended up to 30 days. The LOS data for each basin is presented in (Table 4). The observed extension in the length of the growing season in irrigated areas may have occurred as a result of divergent factors, and needs to be interpreted with caution. While increasing availability of irrigation water and improved agricultural practices (including an “interseason” crop) may be a factor, recent analysis has also highlighted an extended length of season as a result of recurrent droughts in Sri Lanka during the irrigation season (Abeysingha and Rajapaksha, 2020).

67. In order to interpret the potential reasons for the extension in the LOS, a trend analysis has been performed on the NDVI for each basin; droughts (particularly when persistent) would appear as a reduced mean NDVI. Results of the trend analysis show that 12 out of the 25 basins demonstrate a significant increase in NDVI over the 2000 – 2018 period at 95% confidence interval (p -value < 0.05). These basins are identified in the last column of Table 4; for each of these it is unlikely that the extension the LOS is as a result of drought.

Table 4: Change in length of season (LOS) compared over pre-2010 and post-2010-time period and difference in LOS presented for each basin.

Basin	Average LOS (2000-2010)	Average LOS (2011-2018)	LOS extension	NDVI trend increase
Andella Oya	172	168	-4	Yes
Maduru Oya	182	183	1	Yes
Magalavatavan Aru	181	182	1	Yes
Karanda Oya	191	194	3	
Katupila Ara	184	187	3	
Heda Oya	195	198	3	
Karambalan Oya	186	190	3	
Maha Oya	190	194	4	Yes
Mundini Aru	179	184	5	Yes
Kumbukkan Oya	204	211	7	Yes
Gal Oya	182	190	8	Yes
Wila Oya	194	203	9	
Kalagamu Aru	183	193	10	
Mi Oya	188	199	11	
Namadagas Ara	172	185	12	
Deduru Oya	190	202	12	Yes
Rathambala Oya	173	186	13	Yes
Kurunde Ara	167	180	13	
Kala Oya	189	205	16	Yes
Bagura Oya	181	199	18	
Menik Ganga	214	234	20	Yes
Pannala Oya	164	185	22	
Walawe Ganga	204	229	25	Yes
Kirindi Oya	204	230	26	
Malala Oya	198	227	30	
Average	187	198	11	

2. Crop Water Consumption

68. The pySEBAL based analysis (encompassing the estimation of Above Ground Biomass Production (AGBP), and water deficits) has been performed in this study to assist in the identification and prioritization of opportunities to improve the productive use of water through improved supply within the tank systems of selected basins in Sri Lanka.

69. Seasonal water consumption during the Maha and Yala cropping seasons is presented in Figure 13 to Figure 16. These seasonal ETa calculations are based on the cloud free pixels available within each Landsat tile; for the four priority basins cloud cover was persistent during the seasons analyzed (Table 1). It does not include spatial gap filling for the cloud masked areas. Therefore, ETa values may seem lower than expected in

seasonal aggregates, because multiple times within a season the pixels might have been cloud covered and masked out. Moreover, due to the unavailability of cloud free images during the Maha 2018 and the Yala 2015 and 2016 seasons (see Table 2), it was not possible to perform the analysis for these years. While the actual values should thus be treated with caution, the data still provide a spatial overview of relative differences between locations, as well as broad seasonal patterns.

70. Analysis of the data across all four basins highlights a few key points; i) the rainfed cropping region demonstrates a higher seasonal ETa consistently during the Maha season when compared to the Yala (dry) season, ii) the double cropping areas (Figure 7) had consistently higher seasonal ETa, iii) the Maha season of 2015 had higher mean ETa than other years, iv) the Maha seasons of 2017 had lower mean ETa than other years, v) the Yala season demonstrates greater variability in ETa between years as compared to the Maha season.

71. In addition, examining the four basins individually highlights that: i) the 2014 and 2015 Maha season demonstrated higher seasonal ETa in both the Mi Oya and Deduru Oya basins across all cropping systems, while the 2017 Maha season demonstrated lower seasonal ETa for irrigated areas in these basins, and ii) the 2017 Yala season had lower seasonal ETa across the Mi Oya and Deduru Oya basins.

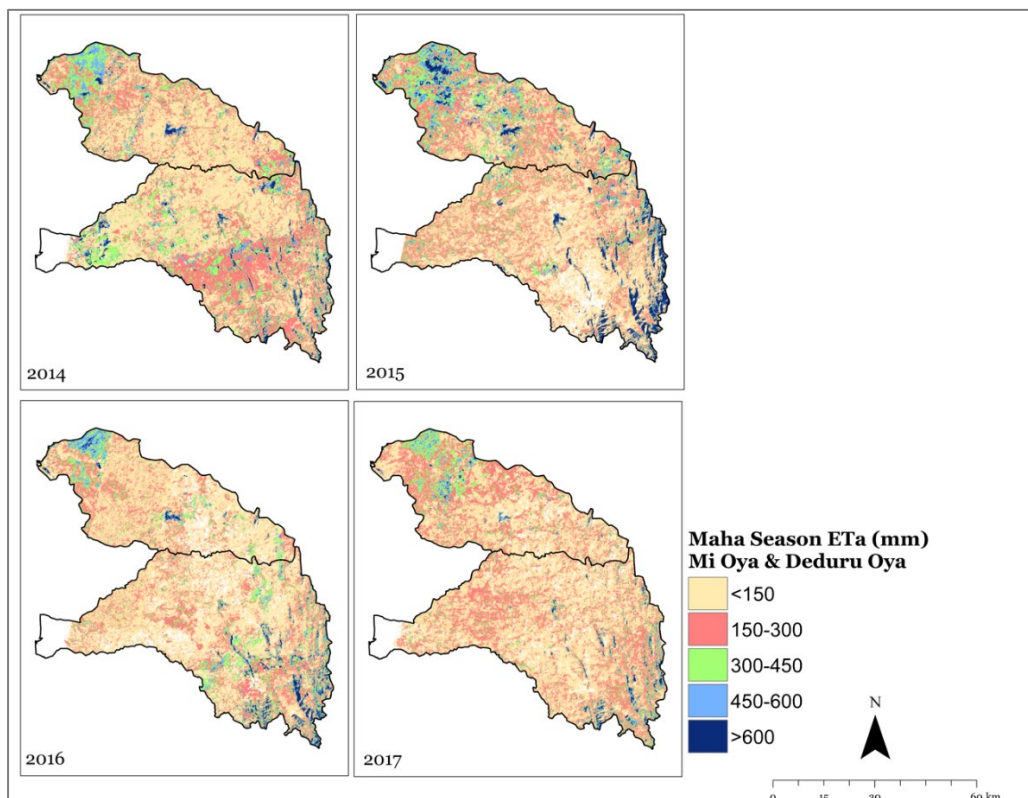


Figure 13: Spatiotemporal distribution of seasonal ETa during the Maha season in the Mi Oya and Deduru Oya.

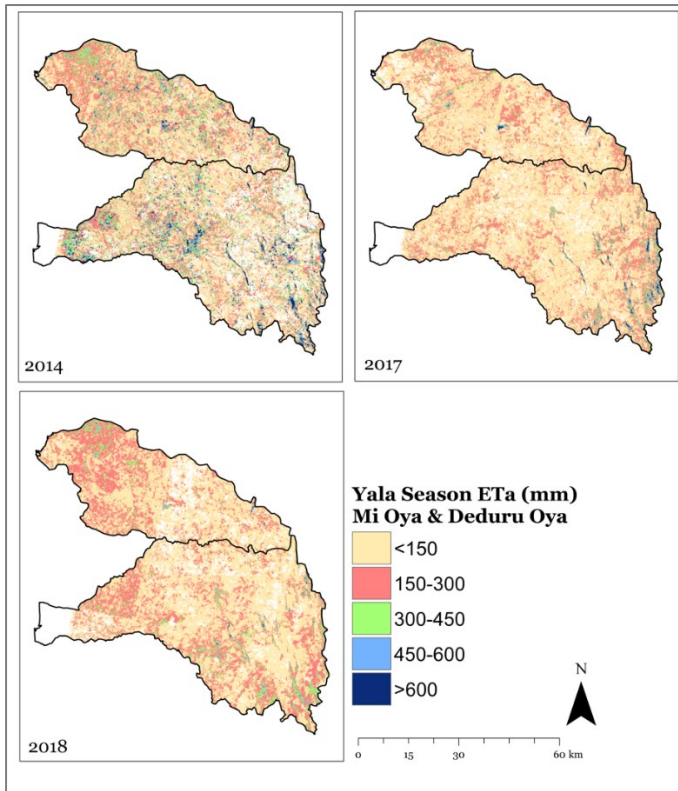


Figure 14: Spatiotemporal distribution of seasonal ETa during the Yala seasons in Mi Oya and Deduru Oya.

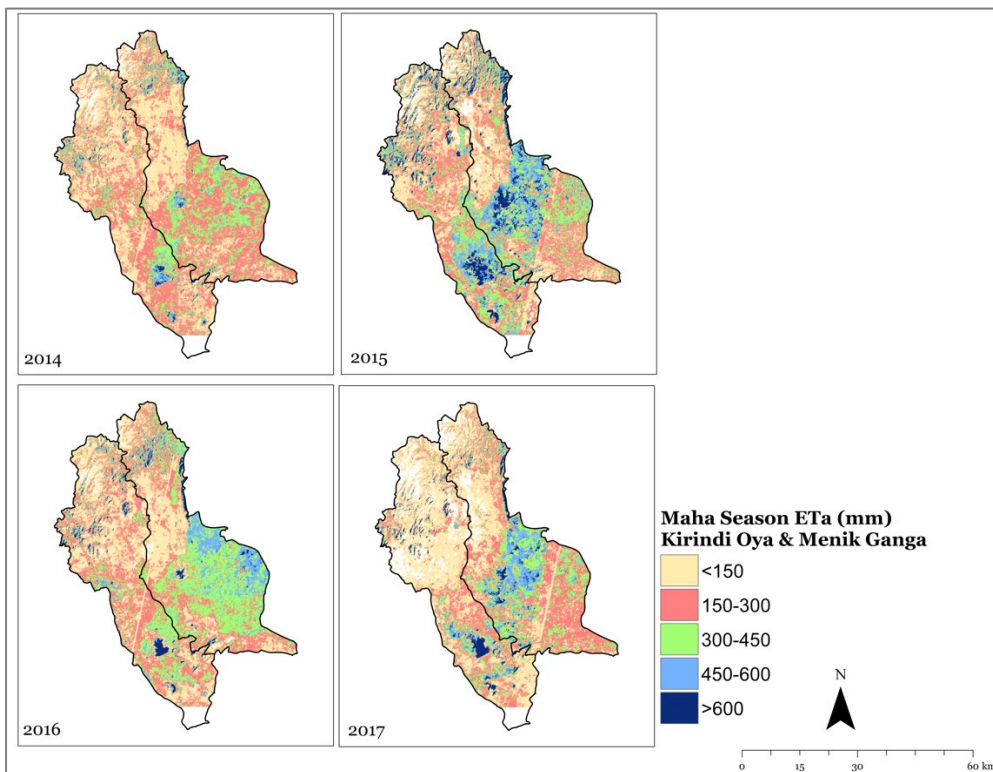


Figure 15: Spatiotemporal distribution of seasonal ETa during Maha season in Kirindi Oya and Menik Ganga.

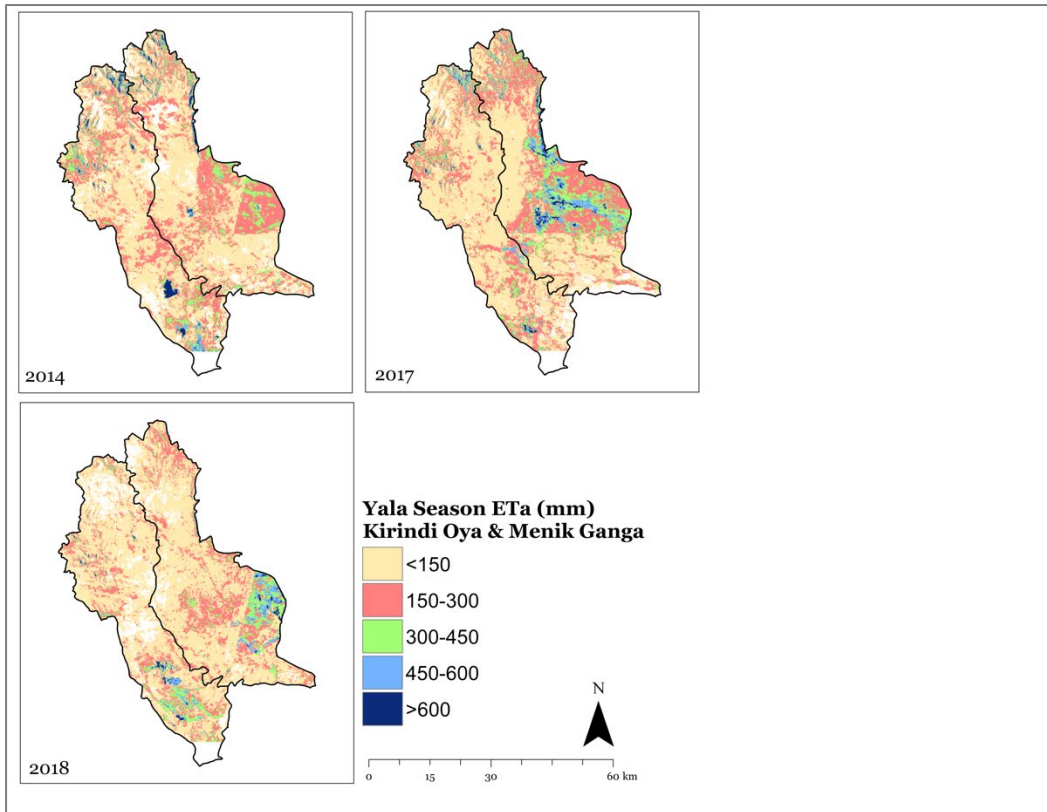


Figure 16: Spatiotemporal distribution of ETa during the Yala season in the Kirindi Oya and Menik Ganga.

3. Relative Water Deficit

72. In order to interpret the spatial distribution of water deficits across the command areas, maps showing the frequency with which a pixel experienced different levels of water deficits (mapped as percentage of deficit days over the Maha and Yala seasons based on the RWD index) are displayed in Figure 17 to Figure 20 for the Mi Oya and Deduru Oya, and the Kirindi Oya and Menik Ganga respectively. The colour indicates the percentage of time a given pixel was deficit.

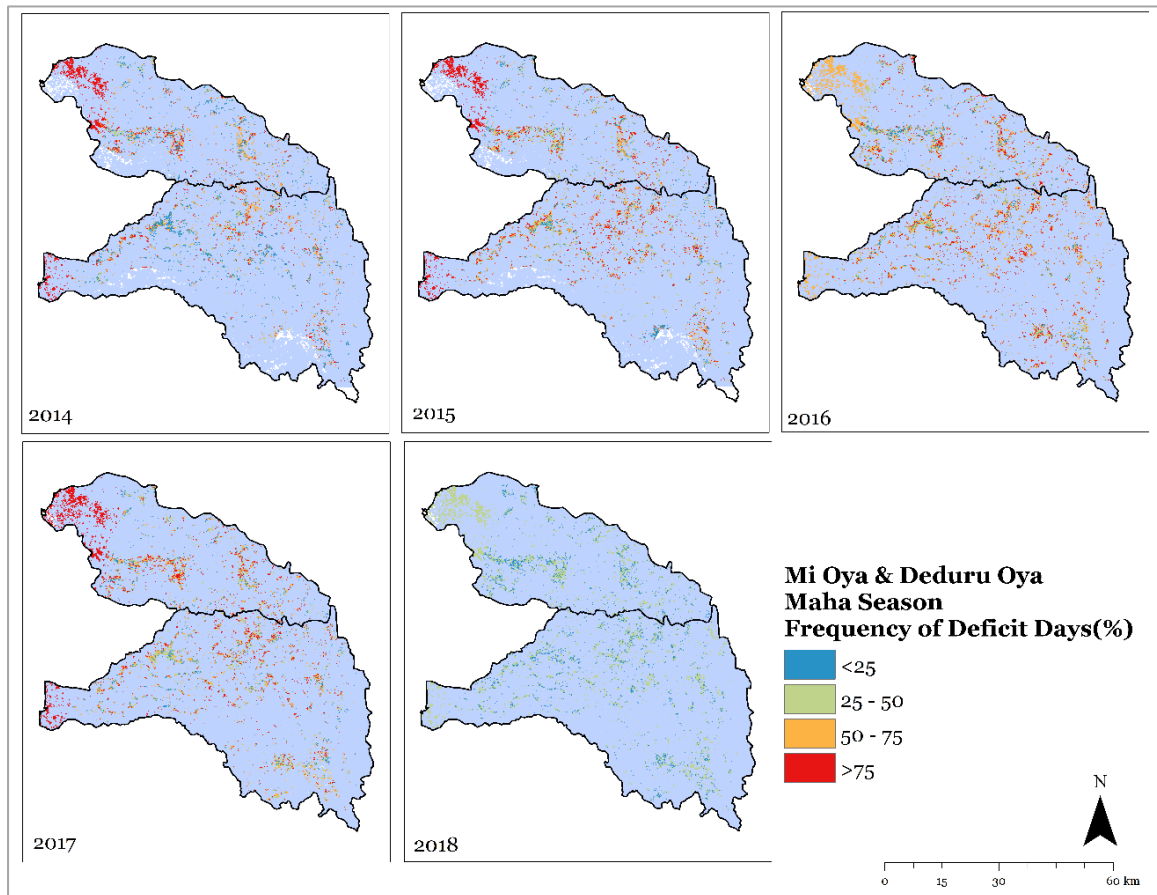


Figure 17: Frequency of water deficits in irrigated areas during the Maha season each year in Mi Oya (top basin) and Deduru Oya (bottom basin).

73. Varying levels of deficit from low, to high, are evident across each basin and each year during the Maha season (Figure 17). It should be noted that for 2018 the data does not cover the entire season as the analysis was only conducted for the first half until January 2019, due to data availability. Hence while useful for identifying spatial patterns, the data should not be compared to the previous years.

74. In both the Mi Oya and Duduru Oya higher deficits are evident at the lower end of the basin (the portions in the west near the coast) for all years except 2016. This pattern is also evident during the drier Yala season (Figure 18). In contrast to the Maha season, more persistent deficits are evident during the Yala season, both spatially and temporally.

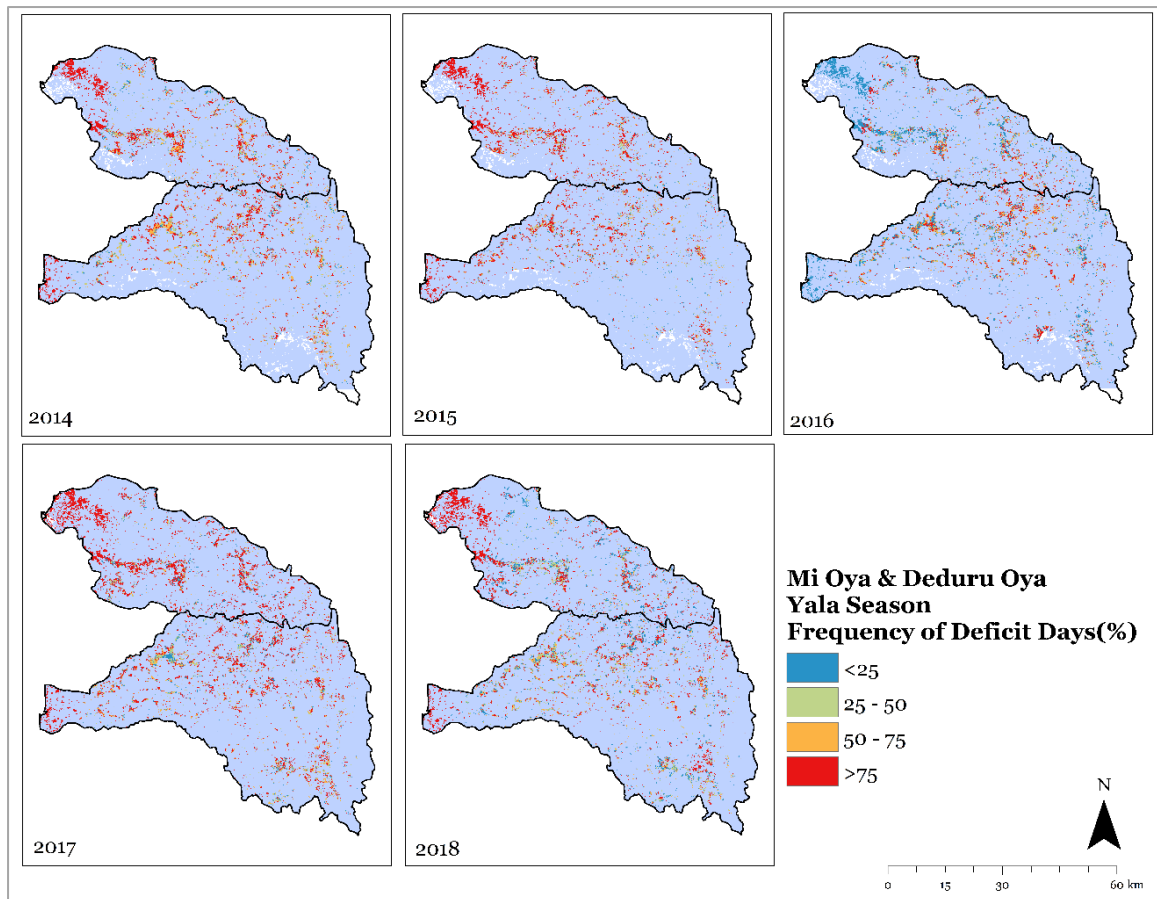


Figure 18: Frequency of water deficits in irrigated areas during the Yala season each year in Mi Oya (top basin) and Deduru Oya (bottom basin).

75. The Kirindi Oya and Menik Ganga basins exhibit more spatially distinct clusters of longer and shorter deficits (Figure 19) than the northern basins. This is likely due to the different nature of the irrigated areas and cropping systems in these basins (see Figure 7) and well as the fact that these two basins are affected by a different monsoon weather pattern than the northern basins. The irrigated double crop regions in the Kirindi Oya (left basin Figure 19), typically demonstrates lower deficits than the irrigated areas in the rest of the basins. In general, less persistent deficits are observed in 2016 and 2017.

76. Overall, both the Kirindi Oya and Menik Ganga exhibit higher deficits during the Yala season (Figure 20) when compared to the Maha season (Figure 19). Following the rainfall distribution, water stress is likely to be highest during the later part of the Yala season (the months of June, July and August). However, given the cloud cover challenges the results are only available for the entire season, rather than monthly, so it is not possible to separate out sections of the season. Within the basins, as with the Maha season, the deficits vary spatially with the irrigated areas in the lower portion of the Kirindi Oya basin (which are located south of a large reservoir) demonstrating less persistence deficits than the rest of the irrigated areas. The 2016 Yala season exhibited extreme deficit across the entire basin; this was a drought year.

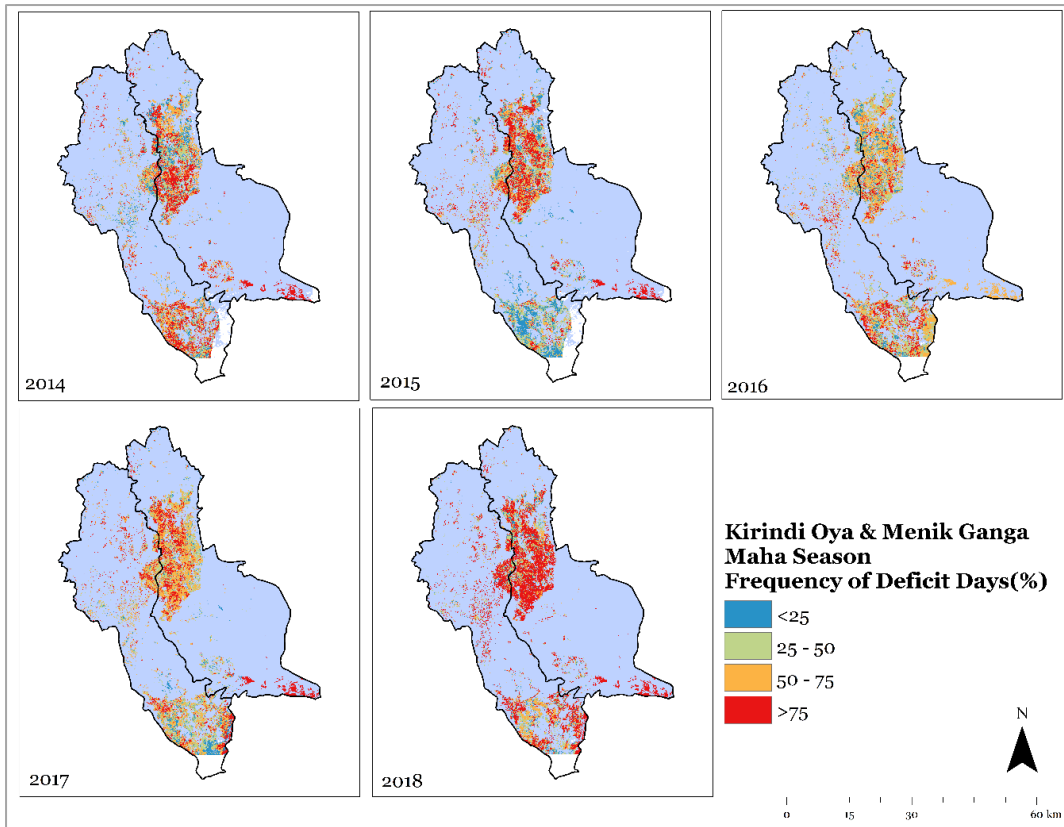


Figure 19: Frequency of water deficits in irrigated areas during the Maha season each year in Kirindi Oya (left basin) and Menik Ganga (right basin)

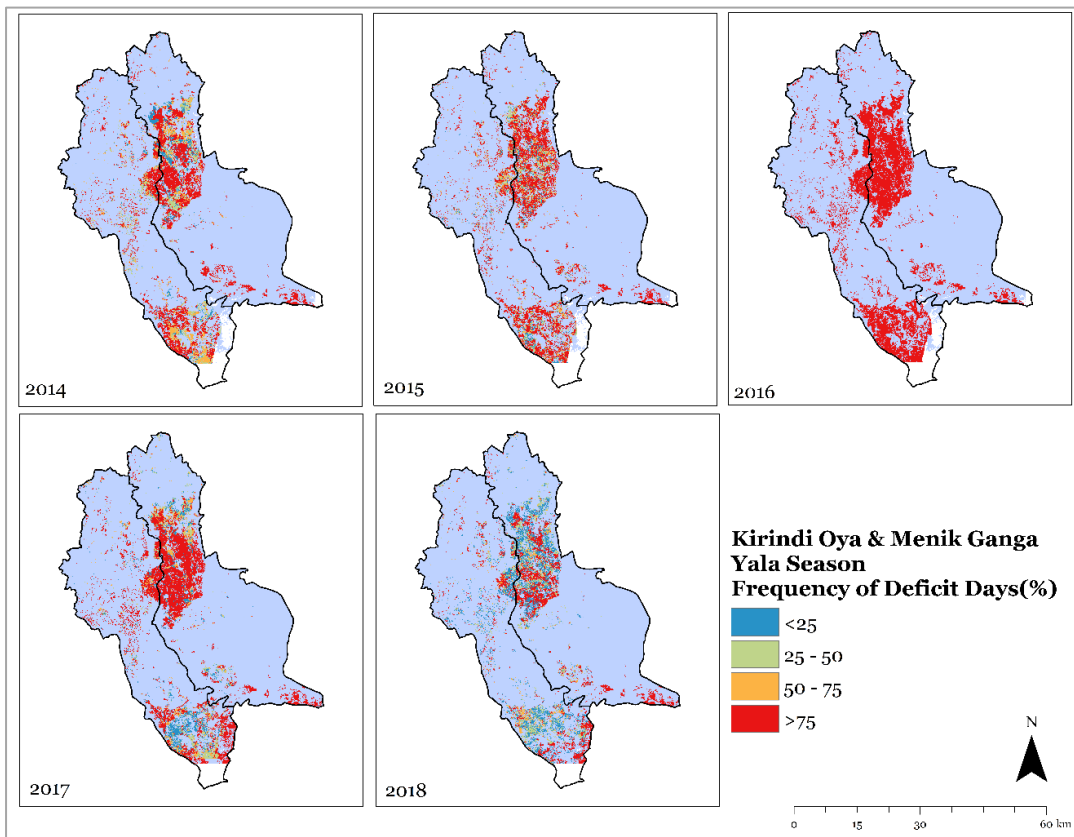


Figure 20: Frequency of water deficits in irrigated areas during the Yala season each year in Kirindi Oya (left basin) and Menik Ganga (right basin).

4. Above Ground Biomass Production

77. AGBP summaries for the Maha season are displayed in Table 5 for irrigated areas in all four basins. These data demonstrate that during the Maha season the AGBP was variable across the basins, with the northern basins (Mi Oya and Deduru Oya) exhibiting higher values for the first 3 years. All four basins show an increasing trend in production over the Maha season over the four-year period, with mean AGBP values increasing between 2014 and 2017. While increases occur in all basins, they are largest for the two southern basins, Kirindi Oya and Menik Ganga; by 2017 all basins show similar mean AGBP in the order of 11,000 kg/ha.

Table 5: Mean AGBP in kg/ha for irrigated areas within each basin for the Maha season

Maha	Mi Oya	Deduru Oya	Kirindi Oya	Menik Ganga
2014	10,816	11,168	8,915	9,230
2015	10,228	11,685	9,892	9,449
2016	10,488	11,806	9,652	9,020
2017	11,936	11,858	11,879	11,340

Table 6: Mean AGBP in kg/ha for irrigated areas within each basin for the Yala season

Yala	Mi Oya	Deduru Oya	Kirindi Oya	Menik Ganga
2014	5,766	6,516	5,016	5,582
2015	9,757	10,484	8,392	8,914
2016	9,699	9,813	6,798	6,577
2017	9,690	9,450	7,397	6,471
2018	8,382	9,099	9,552	9,700

78. AGBP summaries for the drier Yala season (Table 6) demonstrate i) considerably lower production values than during the Maha season, and ii) greater variability from year to year across all four basins. These results are expected given the greater dependency on irrigation water during the Yala season.

79. The AGBP across the irrigated areas of the four basins ranges from a minimum of 5,016 kg/ha during the Yala season, to a maximum of 12,806 kg/ha during the Maha season. In general, the Deduru Oya had higher AGBP estimates and the Kirindi Oya and Menik Ganga had lower AGBP estimates; these findings are in line with the FAO reported mean rice yields from the districts within these basins during the Maha and Yala seasons (FAO 2020).

80. The spatial distribution of the AGBP data are shown in Figure 21 Figure 24. It should be noted that for 2018 the AGBP does not cover the entire Maha season as the analysis was only conducted for the first half until January 2019, due to data availability.

Hence while useful for identifying spatial patterns, the data should not be compared to the previous years.

81. For the northern basins (Mi Oya and Deduru Oya), the locations with higher values (>10,000 kg/ha) are typically located in the irrigated double cropped areas in Figure 7. This is particularly evident in the Deduru Oya basin (Figure 21 and Figure 22) during both seasons. In these basins, 2017 demonstrates higher AGBP values than other years.

82. For the southern basins Kirindi Oya and Menik Ganga (Figure 23 and Figure 24), the highest values are also typically located in the irrigated double cropped areas in Figure 7. In particular, the areas in the lower Kirindi Oya basin, downstream of a large reservoir have consistently higher values than other irrigation areas.

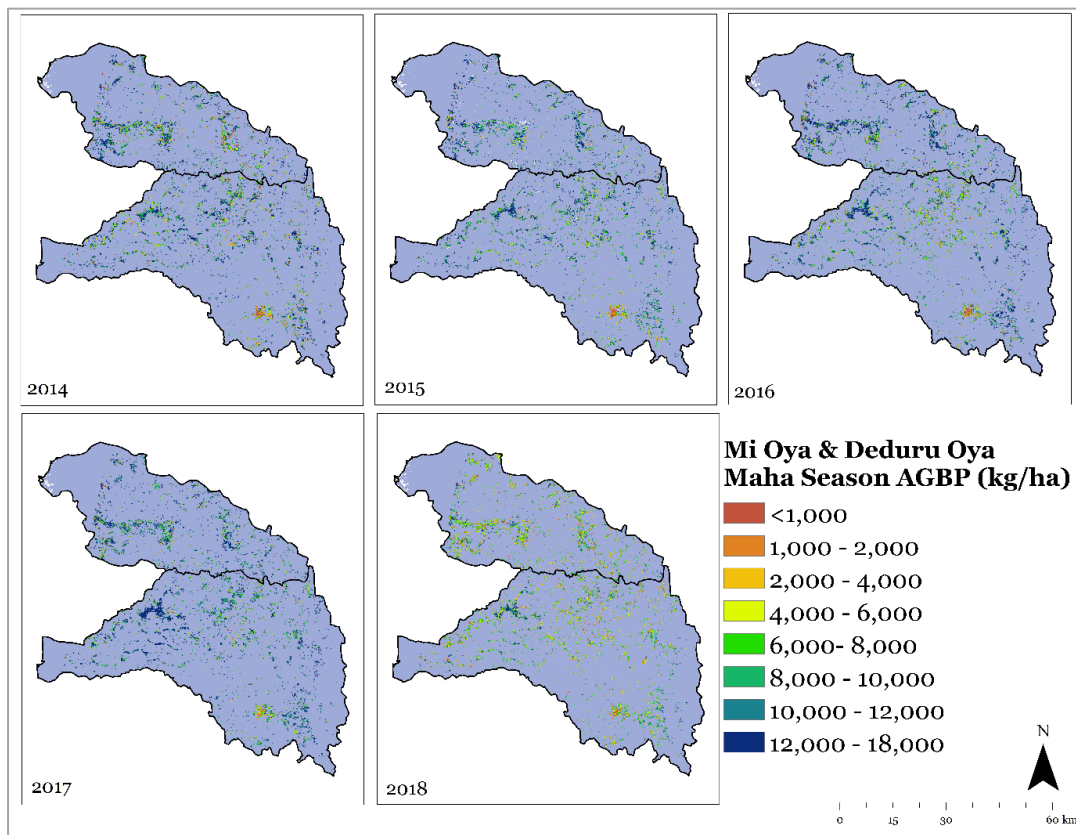


Figure 21: AGBP (kg/ha) for the Maha Season in irrigated areas within the Mi Oya (top basin) and Deduru Oya (bottom basin).

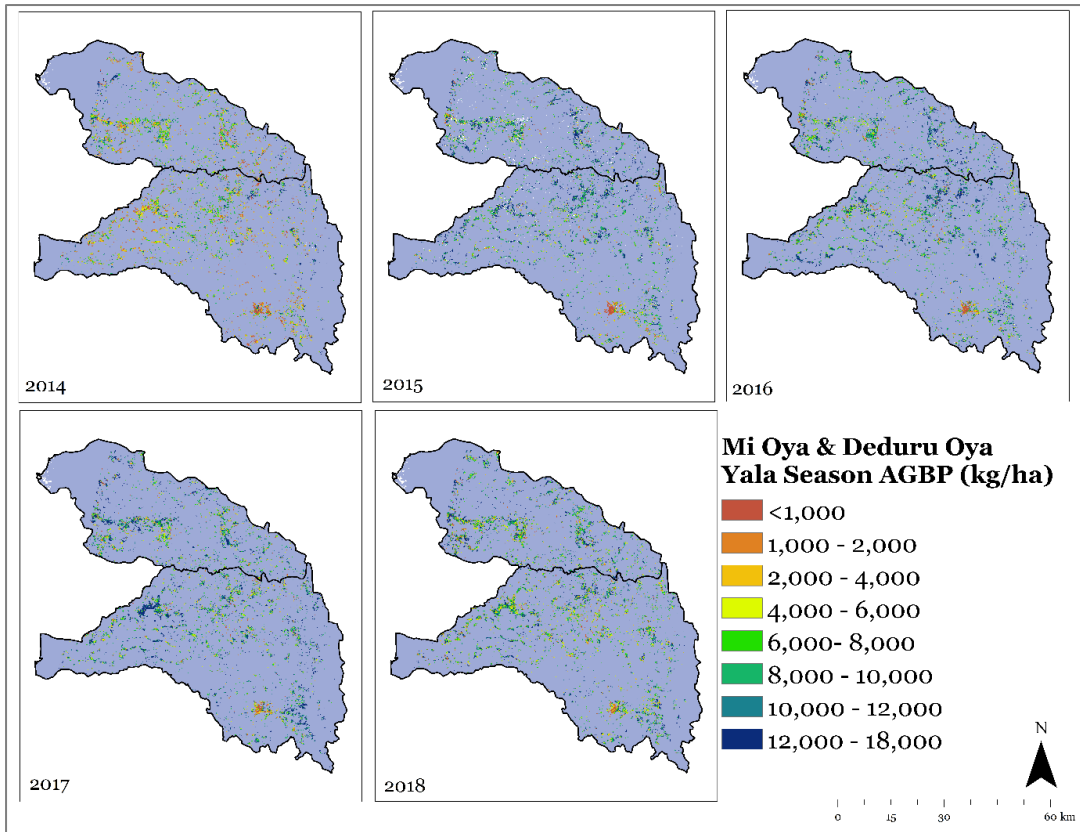


Figure 22: AGBP (kg/ha) estimates for the Yala Season in the irrigated areas of the Mi Oya (top basin) and Deduru Oya (bottom basin).

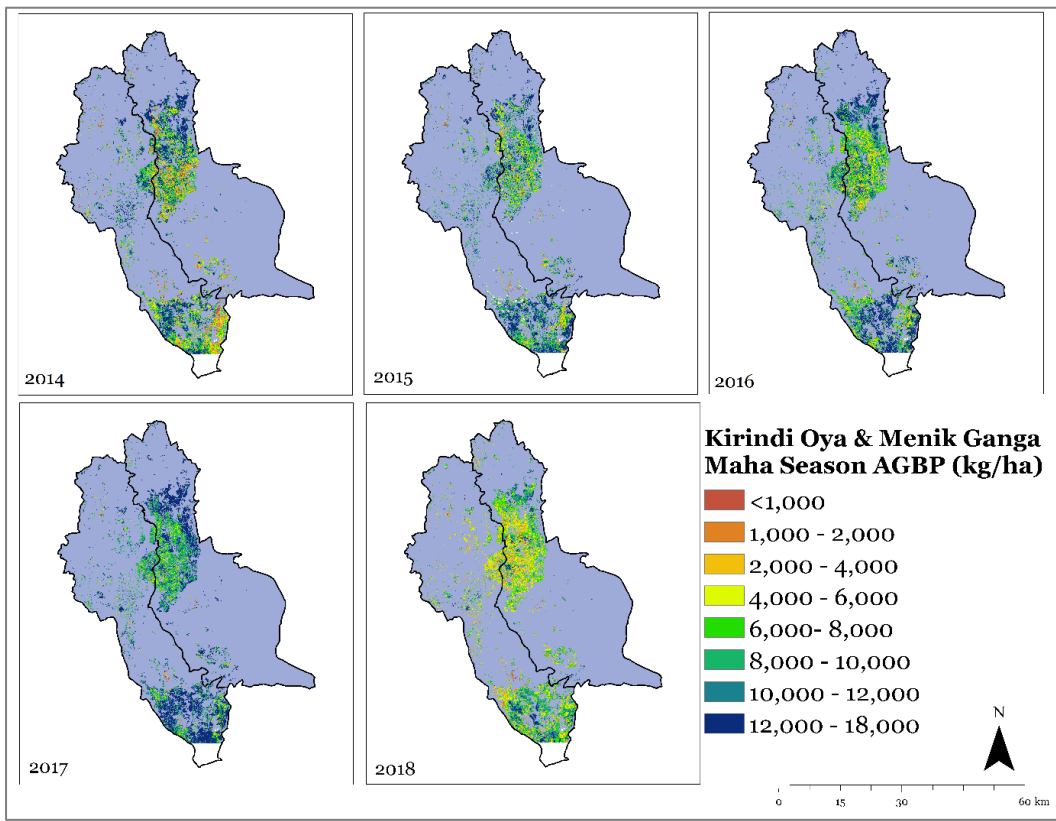


Figure 23: AGBP (kg/ha) for the Maha season in irrigated areas of the Kirindi Oya and Menik Ganga.

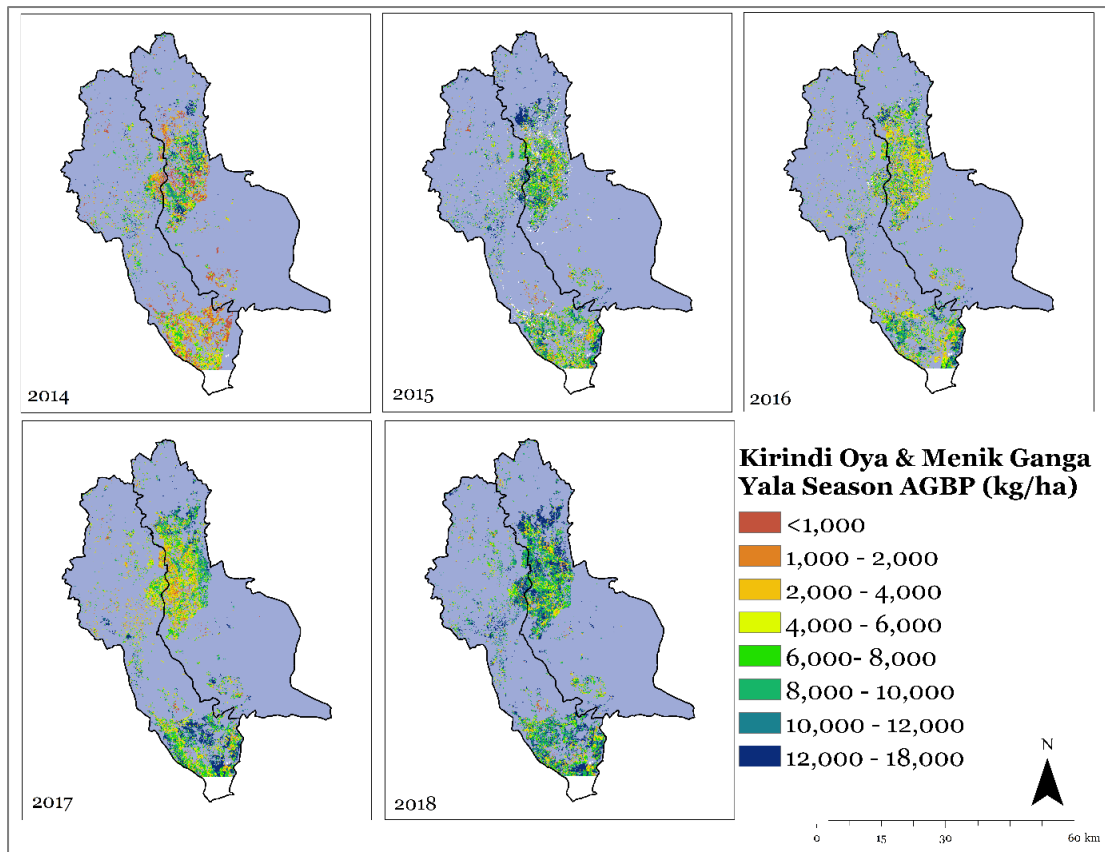


Figure 24: AGBP (kg/ha) for the Yala Season in the irrigated areas of the Kirindi Oya and Menik Ganga.

V. SUMMARY AND KEY FINDINGS

83. In this study, remote sensing techniques have been used to undertake two levels of analysis: 1) lower spatial resolution data has been analyzed over a long time period (18 years, 2000-2018) across 25 river basins to characterise changes and trends in crop phenology, and 2) higher spatial resolution data has been used over a shorter time period (5 years, 2014-2018) across 4 priority river basins to estimate and analyse the water consumed and plant biomass produced. The objective of first level of analysis is intended to support the selection and planning of follow-on river basins, while the objective of the second, more detailed assessment to inform the selection of sub projects within the four priority basins for investment.

84. This report has presented the modelling approach and input data used, and presented the key outputs. A second report (Part B) interprets the results further to meet the second objective. To this end, the data presented in Part A (this report) will be further analyzed against the location of tanks and reservoirs, in order to support the selection of irrigation infrastructure for improvement in part B. Part B investigates potential approaches to link the location of small tank cascades as well as medium and large systems to the water deficit outputs.

85. A large number (337) of Landsat images have been processed for the purpose of this report using the pySEBAL approach. The frequent monsoonal and convectional rainfall events over the island of Sri Lanka has presented a challenge in the acquisition of cloud free images, necessitating the use of images with higher than normally acceptable cloud cover. The results thus need to be used with caution, and analyzed in terms of the relative patterns and extremes presented in the spatial and temporal variables, rather than the specific values.

86. The crop phenology analysis over the full irrigation cropping season (Maha + Yala) over the time period 2000-2018 highlighted several interesting results. The Maha irrigation season started consistently (around mid-October) during the 18-year period, demonstrating low year-to-year variability and no changing trend. However, the end of the season (Yala) was observed to occur around August but demonstrated high variability. Subsequently, a high variability was observed in the total length of the combined Maha and Yala seasons, with an increase in the cropping season by, on average, 11 days over the 18-year period and across all areas. On average, the total length of the irrigation seasons was found to gradually increase since 2010.

87. Out of the 25 river basins, 8 basins (Kalagamu Aru, Mi Oya, Namadagas Ara, Deduru Oya, Rathambala Oya, Kurunde Ara, Kala Oya and Bagura Oya) demonstrated an increase in the LOS of up between 10 and 20 days.

88. Further to this, out of the 25 river basins, 5 basins (Menik Ganga, Pannala Oya, Walawe Ganga, Kirinidi Oya, and Malala Oya) demonstrated an increase in the LOS of greater than 20 days.

89. The observed extension in the length of the growing season in irrigated areas may have occurred as a result of divergent factors, and needs to be interpreted with caution. While increasing availability of irrigation water and improved agricultural practices (including an “interseason” crop) may be a factor, recent analysis has also highlighted an extended length of season as a result of recurrent droughts in Sri Lanka during the irrigation season (Abeysingha and Rajapaksha, 2020). The above results should thus be used as a starting point to guide further assessments.

90. The trend in the NDVI over 2000-2018 was assessed to determine if the extension in LOS was due to drought or other factors. Based on this, 13 river basins are identified where the LOS either remained the same, or the LOS increased but there was no significant increasing trend in the NDVI. These include Karanda Oya, Katupila Ara, Heda Oya, Karambalan Oya, Wila Oya, Kalagamu Aru, Mi Oya, Namadagas Ara, Kurunde Ara, Bagura Oya, Pannala Oya, Kirinidi Oya, and Malala Oya. These basins may be ranked a higher priority for further assessment and potential investment.

91. The data on water deficits for the priority basins shows that in for the northern basins, both the Mi Oya and Deduru Oya exhibit higher deficits in the lower end of the basin (the portions in the west near the coast) for all years except 2016. This pattern is also evident during the drier Yala season. In addition, in contrast to the Maha season, more persistent deficits are evident during the Yala season, both spatially and temporally.

92. The two southern basins, Kirindi Oya and Menik Ganga, exhibit more spatially distinct clusters of longer and shorter deficits than the northern basins. This is likely due to the different nature of the irrigated areas and cropping systems in these basins as well as the fact that these two basins are affected by a different monsoon weather pattern. The irrigated double crop regions in the Kirindi Oya typically demonstrates lower deficits than the irrigated areas in the rest of the basin. In general, less persistent deficits are observed in 2016 and 2017.

93. Overall, both the Kirindi Oya and Menik Ganga exhibit higher deficits during the Yala season when compared to the Maha season, although the deficits vary spatially with the irrigated areas in the lower portion of the Kirindi Oya basin (located south of a large reservoir) demonstrating less persistent deficits than the rest of the irrigated areas. The 2016 Yala season exhibited extreme deficit across the entire basin; this was a drought year.

VI. REFERENCES

- Abeysingha, N.S., Jayasekara, J., Meegastenna, T.J. (2017). Stream flow trends in up and midstream of Kirindi Oya river basin In Sri Lanka and its linkages to rainfall. *Mausam*, 68, 99-110.
- Abeysingha, N.S., Rajapaksha, U.R.L.N. (2020). SPI-Based Spatiotemporal Drought over Sri Lanka. *Advances in Meteorology*, 2020.
- Allen, R.G., Pereira, L.S., Howell, T.A., Jensen, M.E. (2011). Evapotranspiration information reporting: I. Factors governing measurement accuracy. *Agricultural Water Management*, 98(6), 899-920.
- Bastiaanssen, W.G. (2000). SEBAL-based sensible and latent heat fluxes in the irrigated Gediz Basin, Turkey. *Journal of hydrology*, 229(1-2), 87-100.
- Bastiaanssen, W.G., Chandrapala, L. (2003). Water balance variability across Sri Lanka for assessing agricultural and environmental water use. *Agricultural water management*, 58(2), 171-192.
- Bastiaanssen, W.G., Menenti, M., Feddes, R.A., Holtslag, A.A.M. (1998). A remote sensing surface energy balance algorithm for land (SEBAL). 1. Formulation. *Journal of hydrology*, 212, 198-212.
- Dissanayake, P., Smakhtin, V. (2007). Environmental and social values of river water: Examples from the Menik Ganga, Sri Lanka (Vol. 121). IWMI.
- Eriyagama, N., Smakhtin, V., Jinapala, K. (2015). The Sri Lanka environmental flow calculator: A science-based tool to support sustainable national water management. *Water Policy*. 18. 10.2166/wp.2015.158.
- FAO (2019). "Sri Lanka: Rivers". Retrieved 16 June 2019 <http://www.fao.org/3/T0028E/T0028E02.htm>.
- FAO 2020. Accessed at <http://www.fao.org/3/x6905e/x6905e0c.htm> on October 2020.
- Forkel, M., Wutzler, T. (2015). Greenbrown-land surface phenology and trend analysis. A package for the R software. *Version*, 2, 2015-04.
- IHE Delft and IWMI, 2020. *Water Productivity and Water Accounting: Methodology Manual*. Delft, The Netherlands.
- Irmak, A., Allen, R.G., Kjaersgaard, J., Huntington, J., Kamble, B., Trezza, R., Ratcliffe, I. (2012). Operational remote sensing of ET and challenges. *Evapotranspiration—Remote Sensing and Modeling*, 467-492.

IWMI, 2013. Spatial Database for Climate Change Vulnerability Mapping in South Asia (<https://ccafs.cgiar.org/blog/newly-developed-irrigation-map-south-asia-presented#.XvjSSedS9EZ>).

Jayawardhana, W.G.N.N., Chathurange, V.M.I. (2016). Extraction of agricultural phenological parameters of Sri Lanka using MODIS, NDVI time series data. *Procedia food science*, 6, 235-241.

Karimi, P., Bastiaanssen, W.G. (2015). Spatial evapotranspiration, rainfall and land use data in water accounting--Part 1: Review of the accuracy of the remote sensing data. *Hydrology & Earth System Sciences*, 19(1).

Nugent, J. (2018). Cloudy with a chance of "cirrus" science. *Science Scope*, 42(2), 26-28.

Samarasinghe, S.A.P., Sakthivadivel, R., Sally, H. (2000). Sustainable management of the Deduru Oya River Basin, Sri Lanka: A case study of institutions, organizations and actors. A Working Paper of South Asia Regional Workshop on River Basin Management. Colombo, Sri Lanka. Retrieved 15th May, 2012 from http://publications.iwmi.org/pdf/H_30853.pdf.

Wickramaarachchi, T.N. (2004). Preliminary assessment of surface water resources-a study from Deduru Oya Basin of Sri Lanka. APHW Proceedings. <http://rwes.dpri.kyoto-u.ac.jp/~tanaka/APHW/APHW2004/proceedings/OHS/56-OHS-A341/56-OHS-A341.pdf>.

Wijesekera, S. (2015). Irrigated Paddy Cultivation Systems in Sri Lanka and Climate Change: Indifference or as a Crucial Element.